

UNCONDITIONAL FULL LINEAR CONVERGENCE AND QUASI-OPTIMAL COMPLEXITY OF SMOOTHED ADAPTIVE FINITE ELEMENT METHODS

PHILIPP BRINGMANN , CHRISTOPH LIETZ , AND DIRK PRAETORIUS 

ABSTRACT. We present the first rigorous convergence analysis of the smoothed adaptive finite element method (S-AFEM) proposed in [Mulita, Giani, Heltai: SIAM J. Sci. Comput. 43, 2021]. S-AFEM modifies the classical adaptive finite element method (AFEM) by performing accurate discrete solves only on periodically determined mesh levels, while the intermediate levels employ a fixed number of cheap smoothing iterations. Numerical experiments in that work showed that this strategy generates adapted meshes comparable to those of AFEM at substantially lower computational cost. In this paper, we prove unconditional full R-linear convergence of a suitable quasi-error quantity and, for sufficiently small adaptivity parameters, optimal convergence rates with respect to the overall computational cost. The analysis requires only a mild uniform stability assumption on the employed smoother, satisfied by standard methods such as Richardson, Gauss–Seidel, conjugate gradient, and multigrid schemes. Our results apply to general second-order linear elliptic PDEs and show that S-AFEM retains all desired abstract convergence guarantees of AFEM while reducing the cumulative computational time. Numerical experiments validate the theory, analyze runtime performance, and underline the potential of S-AFEM for speed-up in AFEM computations.

1. INTRODUCTION

Motivation and overview. The ultimate goal of any numerical method for partial differential equations (PDEs) is to approximate the exact solution with quasi-minimal computational cost. Adaptive finite element methods (AFEMs) achieve this by iteratively steering the mesh refinement based on a *posteriori* refinement indicators and a marking strategy. The smoothed adaptive finite element method (S-AFEM), introduced in [MGH21], is a practice-oriented variant of AFEM designed to significantly reduce the number of expensive discrete solves within the adaptive loop. It is motivated by the key observation that a few iterations of a cheap smoother already yield refinement indicators close to those obtained with the exact discrete solution; see [Figure 1](#). S-AFEM modifies the classical AFEM loop in that accurate discrete solutions are computed only on periodically determined levels of the mesh hierarchy. The intermediate levels employ a fixed number of inexpensive smoothing steps. Extensive numerical experiments in [MGH21] demonstrate that this strategy produces mesh sequences that closely resemble those of classical AFEM, but at significantly reduced computational cost. A rigorous convergence analysis of S-AFEM, however, has been missing so far.

Algorithmically, the method inserts a cheap **SMOOTH** module into the classical AFEM loop, replacing **SOLVE** on intermediate levels; see [Figure 2](#). The classical AFEM loop in [Figure 2](#) generates a sequence of meshes $(\mathcal{T}_\ell)_{\ell \in \mathbb{N}_0}$ and corresponding finite element approximations $(u_\ell)_{\ell \in \mathbb{N}_0}$ to the exact continuous solution u^* . On each mesh \mathcal{T}_ℓ , the **SOLVE** module computes an *accurate* approximation u_ℓ of the exact discrete solution u_ℓ^* . The **ESTIMATE** module then evaluates computable refinement indicators $\eta_\ell(T, u_\ell) \geq 0$ for each element $T \in \mathcal{T}_\ell$ to estimate the local contribution to the overall *a posteriori* error estimator $\eta_\ell(u_\ell)$. Based on these indicators, the

2010 *Mathematics Subject Classification.* 65N30, 65N50, 65N15, 65Y20, 41A25, 65F10.

Key words and phrases. adaptive mesh refinement, smoothed adaptive finite element method, full linear convergence, quasi-optimal complexity, second-order elliptic PDEs, iterative solvers.

Acknowledgment. This research was funded in whole or in part by the Austrian Science Fund (FWF) [[10.55776/F65](#), [10.55776/PAT3699424](#), and [10.55776/PAT3446525](#)]. Additionally, Christoph Lietz is supported by the Vienna School of Mathematics.

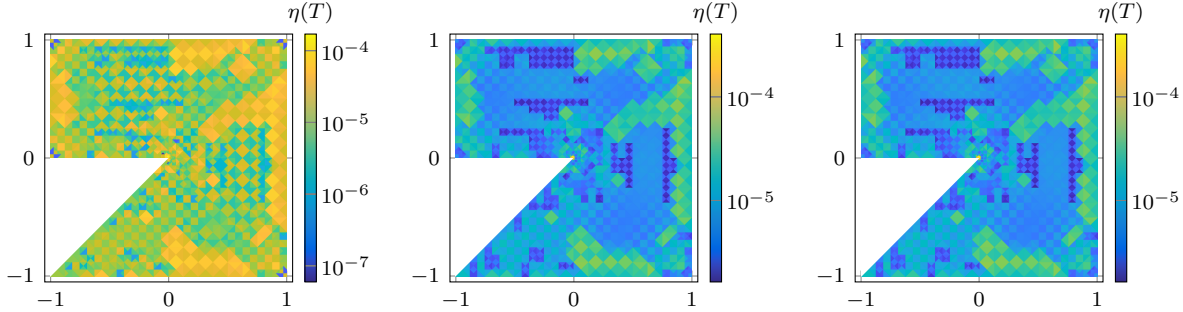


FIGURE 1. Refinement indicators for a Poisson problem for an initial approximation (left), three Gauss–Seidel iterations (center), and the exact discrete solution (right).

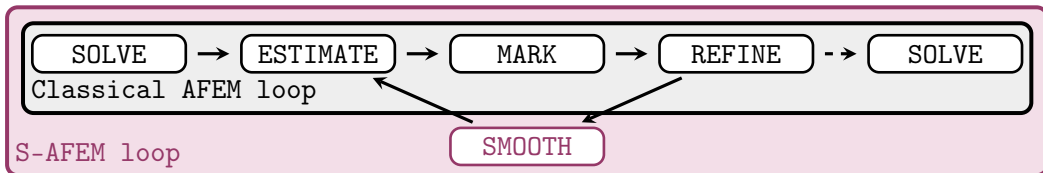


FIGURE 2. Illustration of adaptive refinement loops.

MARK module selects a subset of elements with comparatively large indicators for refinement, and REFINE generates a new mesh $\mathcal{T}_{\ell+1}$ by refining (at least) these marked elements.

S-AFEM alters this algorithm by fixing a period $L \in \mathbb{N}$ and performing SOLVE only on every L -th mesh, resulting in the S-AFEM loop illustrated in Figure 2. On the intermediate mesh levels, SOLVE is replaced by the SMOOTH module consisting of a small number of iterations of a computationally very cheap smoother. Although such smoothers efficiently damp only selected error components and do not aim to fully solve the discrete problem, the resulting refinement indicators remain effective to steer the mesh refinement (cf. Figure 1).

State of the art. The mathematical analysis of the classical AFEM loop in Figure 2 has developed substantially over the past three decades; see, for instance, [Dör96; MNS00; BDD04; Ste07; Ste08; CKNS08; CN12; FFP14] for linear elliptic PDEs, [Vee02; DK08; BDK12; GMZ12] for certain nonlinear PDEs, and [CFPP14] for an abstract axiomatic framework. These contributions establish plain convergence [Dör96; MNS00; Vee02; DK08; GMZ12] as well as optimal convergence rates with respect to the number of degrees of freedom [BDD04; CKNS08; CN12; BDK12; GMZ12; FFP14]. Since AFEM proceeds iteratively, however, optimality should be measured in terms of the overall computational cost (resp. cumulative computation time) rather than the number of degrees of freedom alone. This notion, referred to as *quasi-optimal complexity*, was originally developed for adaptive wavelet methods [CDD01; CDD03] and later extended to AFEM in [Ste07; CG12] under the assumption that the inexact solver is sufficiently accurate.

The works [GHP21; BFM⁺25] employ a uniformly contractive iterative solver computing inexact approximations $u_\ell^k \approx u_\ell^*$ on each mesh \mathcal{T}_ℓ for solver iterations $k = 1, \dots, \underline{k}[\ell]$. The solver is terminated using a stopping criterion that controls the algebraic error relative to the discretization error via a parameter $\lambda > 0$. For general second-order linear elliptic PDEs, [BFM⁺25] establishes *unconditional full R-linear convergence* of the quasi-error $H_\ell^k := \|u_\ell^* - u_\ell^k\| + \eta_\ell(u_\ell^*)$. That is, for arbitrary $\lambda > 0$, the quasi-error H_ℓ^k converges R-linearly with respect to the lexicographic order $|\ell, k| \in \mathbb{N}_0$ for index pairs $(\ell, k) \in \mathbb{N}_0^2$ appearing in the algorithm (collected in the index set \mathcal{Q}), i.e.,

$$H_\ell^k \leq C_{\text{lin}} q_{\text{lin}}^{|\ell, k| - |\ell', k'|} H_{\ell'}^{k'} \quad \text{for all } (\ell', k'), (\ell, k) \in \mathcal{Q} \text{ with } |\ell', k'| \leq |\ell, k|. \quad (1)$$

Moreover, [GHP21] identifies (1) as a key ingredient for proving quasi-optimal complexity for sufficiently small $\lambda > 0$. Formally, quasi-optimal complexity asserts decay of the quasi-error at the largest possible convergence rate $s > 0$ with

$$\sup_{(\ell,k) \in \mathcal{Q}} \left(\sum_{\substack{(\ell',k') \in \mathcal{Q} \\ |\ell',k'| \leq |\ell,k|}} \# \mathcal{T}_{\ell'} \right)^s H_{\ell}^k < +\infty.$$

Since all modules of the adaptive loop in Figure 2 can usually be realized with linear complexity $\mathcal{O}(\# \mathcal{T}_{\ell})$, this notion indeed guarantees optimal convergence rates with respect to the overall computational cost, i.e., optimal complexity.

Main results and contributions. In the present work, we establish the first convergence analysis of the S-AFEM loop shown in Figure 2 with fixed period $L \in \mathbb{N}$, which we call the S-AFEM algorithm. We prove that, despite including smoothing on intermediate mesh levels, S-AFEM still satisfies all abstract convergence guarantees known for AFEM with inexact solvers. In particular, we show that S-AFEM ensures *unconditional full R-linear convergence* (1). Moreover, by introducing a novel cardinality-control step that limits the number of marked elements on intermediate mesh levels, we prove *quasi-optimal complexity* of S-AFEM for sufficiently small adaptivity parameters. Our analysis requires only a mild *uniform stability* assumption on the smoother used in SMOOTH. This assumption is satisfied by standard smoothers such as Richardson, Gauss–Seidel, and conjugate gradient (CG) iterations, as well as by more advanced methods like preconditioned CG and multigrid methods. On the periodically occurring SOLVE levels, we employ a uniformly contractive iterative solver with the stopping criterion from [GHP21]. Crucially, the analysis imposes no restrictions on the choice of the period L or on the number of smoothing iterations performed on intermediate levels. While [LZ21; LS25] construct a *posteriori* error estimators based on smoothers, we steer the mesh refinement with the standard residual-based estimator.

Outline. The remainder of this work is structured as follows. Section 2 presents the model problem of a general second-order linear elliptic PDE, the mesh-refinement framework, and the discrete formulation. It also recalls the residual-based error estimator [AO00; Ver13], the axioms of adaptivity [CFPP14], and the quasi-orthogonality from [Fei22]. Section 3 introduces a broad class of examples for uniformly stable smoothers and shows how Zarantonello symmetrization enables the construction of such smoothers also for non-symmetric problems. Section 4 formalizes the S-AFEM loop shown in Figure 2 in Algorithm A. The main contributions follow thereafter: Section 5 establishes full R-linear convergence of Algorithm A, first unconditionally in Theorem 6 and later, in Theorem 12, under an even weaker assumption on the smoother but for a sufficiently small solver stopping parameter $\lambda > 0$. Section 6 shows in Theorem 14 that the algorithm attains quasi-optimal complexity. Finally, section 7 presents numerical experiments that confirm the theoretical results and analyze the runtime performance of S-AFEM.

2. PRELIMINARIES

2.1. Model problem. Let $\Omega \subset \mathbb{R}^d, d \geq 1$ be a bounded polyhedral Lipschitz domain. Let $\mathbf{A} \in W^{1,\infty}(T; \mathbb{R}_{\text{sym}}^{d \times d})$ and $\mathbf{f} \in W^{1,\infty}(T; \mathbb{R}^d)$ be piecewise Lipschitz-continuous with respect to each element $T \in \mathcal{T}_0$ of an initial triangulation \mathcal{T}_0 of Ω (cf. subsection 2.2). Moreover, let $\mathbf{b} \in L^\infty(\Omega; \mathbb{R}^d)$, $c \in L^\infty(\Omega)$, and $f \in L^2(\Omega)$. The second-order linear elliptic model problem seeks $u^* \in H_0^1(\Omega)$ such that

$$-\operatorname{div}(\mathbf{A} \nabla u^*) + \mathbf{b} \cdot \nabla u^* + cu^* = f - \operatorname{div} \mathbf{f} \text{ in } \Omega \quad \text{subject to} \quad u^* = 0 \text{ on } \partial\Omega. \quad (2)$$

The bilinear form

$$b(v, w) := (\mathbf{A} \nabla v, \nabla w)_{L^2(\Omega)} + (\mathbf{b} \cdot \nabla v + cv, w)_{L^2(\Omega)} \quad (3)$$

is assumed to fit into the Lax–Milgram setting, i.e., there exist constants $C_{\text{ell}}, C_{\text{bnd}} > 0$ such that, for all $v, w \in H_0^1(\Omega)$,

$$C_{\text{ell}} \|v\|_{H^1(\Omega)}^2 \leq b(v, v) \quad \text{and} \quad b(v, w) \leq C_{\text{bnd}} \|v\|_{H^1(\Omega)} \|w\|_{H^1(\Omega)}. \quad (4)$$

Due to (4), the weak formulation of (2) has a unique solution $u^* \in H_0^1(\Omega)$ satisfying

$$b(u^*, v) = (f, v)_{L^2(\Omega)} + (\mathbf{f}, \nabla v)_{L^2(\Omega)} =: F(v) \quad \text{for all } v \in H_0^1(\Omega). \quad (5)$$

The symmetric part $a(\cdot, \cdot)$ of $b(\cdot, \cdot)$ is defined via $a(v, w) := [b(v, w) + b(w, v)]/2$. It satisfies the same ellipticity and continuity bounds as in (4) with $b(\cdot, \cdot)$ replaced by $a(\cdot, \cdot)$ and identical constants C_{ell} and C_{bnd} . Hence, $a(\cdot, \cdot)$ defines an equivalent scalar product on $H_0^1(\Omega)$ and the induced energy norm $\|v\| := a(v, v)^{1/2} = b(v, v)^{1/2}$ is equivalent to $\|\cdot\|_{H^1(\Omega)}$ on $H_0^1(\Omega)$.

2.2. Triangulations and refinement. Let \mathcal{T}_0 be an initial conforming triangulation of Ω into compact simplices. Newest-vertex bisection (NVB) is employed as refinement strategy [Ste08; KPP13; AFF⁺13; DGS25], yielding uniformly shape-regular meshes. For any conforming triangulation \mathcal{T}_H and any $\mathcal{M}_H \subseteq \mathcal{T}_H$, let $\text{refine}(\mathcal{T}_H, \mathcal{M}_H) =: \mathcal{T}_h$ denote the coarsest NVB refinement of \mathcal{T}_H such that at least every marked element is refined, i.e., $\mathcal{M}_H \subseteq \mathcal{T}_H \setminus \mathcal{T}_h$. Define $\text{refine}(\mathcal{T}_H)$ to be the set of all conforming triangulations obtainable from \mathcal{T}_H by finitely many NVB refinements, and $\mathbb{T} := \text{refine}(\mathcal{T}_0)$.

2.3. Discretization. Let $p \in \mathbb{N}$ be a fixed polynomial degree. For each $\mathcal{T}_H \in \mathbb{T}$, define the conforming Lagrange finite element space $\mathcal{X}_H \subset H_0^1(\Omega)$ of degree p by

$$\mathcal{X}_H := \{v_H \in H_0^1(\Omega) \mid \forall T \in \mathcal{T}_H: v_H|_T \text{ is a polynomial of total degree } \leq p\}. \quad (6)$$

This ensures nestedness of the discrete spaces, i.e., $\mathcal{T}_h \in \text{refine}(\mathcal{T}_H)$ implies $\mathcal{X}_H \subseteq \mathcal{X}_h$. For every $\mathcal{T}_H \in \mathbb{T}$, there exists a unique discrete Galerkin solution $u_H^* \in \mathcal{X}_H$ solving

$$b(u_H^*, v_H) = F(v_H) \quad \text{for all } v_H \in \mathcal{X}_H. \quad (7)$$

2.4. Error estimator. For each mesh $\mathcal{T}_H \in \mathbb{T}$ and for all $T \in \mathcal{T}_H$ and $v_H \in \mathcal{X}_H$, we employ the residual-based error estimator [AO00; Ver13] with local contributions

$$\begin{aligned} \eta_H(T, v_H)^2 &:= |T|^{2/d} \| -\operatorname{div}(\mathbf{A} \nabla v_h - \mathbf{f}) + \mathbf{b} \cdot \nabla v_H + cv_h - f \|_{L^2(T)}^2 \\ &\quad + |T|^{1/d} \|[(\mathbf{A} \nabla v_H - \mathbf{f}) \cdot \mathbf{n}]\|_{L^2(\partial T \cap \Omega)}^2, \end{aligned} \quad (8)$$

where \mathbf{n} denotes the outer unit normal vector on ∂T and $\llbracket \cdot \rrbracket$ denotes the jump across $(d-1)$ -dimensional hyperfaces. For any $\mathcal{U}_H \subseteq \mathcal{T}_H$, set

$$\eta_H(\mathcal{U}_H, v_H) := \left(\sum_{T \in \mathcal{U}_H} \eta_H(T, v_H)^2 \right)^{1/2} \quad \text{and} \quad \eta_H(v_H) := \eta_H(\mathcal{T}_H, v_H). \quad (9)$$

Following [CFPP14], the estimator (8) satisfies the *axioms of adaptivity* stated below.

Proposition 1 (axioms of adaptivity). *There exist $C_{\text{stab}}, C_{\text{rel}}, C_{\text{drel}} > 0$, $0 < q_{\text{red}} < 1$, and $C_{\text{mon}} \geq 1$ such that, for any $\mathcal{T}_H \in \mathbb{T}$, any $\mathcal{T}_h \in \text{refine}(\mathcal{T}_H)$, any $\mathcal{U}_H \subseteq \mathcal{T}_H \cap \mathcal{T}_h$, and arbitrary $v_H \in \mathcal{X}_H$, $v_h \in \mathcal{X}_h$, the following properties hold:*

- (A1) **Stability:** $|\eta_h(\mathcal{U}_H, v_h) - \eta_H(\mathcal{U}_H, v_H)| \leq C_{\text{stab}} \|v_h - v_H\|$.
- (A2) **Reduction:** $\eta_h(\mathcal{T}_h \setminus \mathcal{T}_H, v_H) \leq q_{\text{red}} \eta_H(\mathcal{T}_H \setminus \mathcal{T}_h, v_H)$.
- (A3) **Reliability:** $\|u^* - u_H^*\| \leq C_{\text{rel}} \eta_H(u_H^*)$.
- (A3⁺) **Discrete reliability:** $\|u_H^* - u_H^*\| \leq C_{\text{drel}} \eta_H(\mathcal{T}_H \setminus \mathcal{T}_h, u_H^*)$.
- (QM) **Quasi-monotonicity:** $\eta_h(u_h^*) \leq C_{\text{mon}} \eta_H(u_H^*)$.

The constant C_{rel} depends only on the dimension d and uniform shape regularity, while C_{stab} and C_{drel} additionally depend on the polynomial degree p . Moreover, there hold $q_{\text{red}} \leq 2^{-1/(2d)}$ and $C_{\text{mon}} \leq 1 + C_{\text{stab}} C_{\text{drel}}$.

To compensate for the absence of Pythagoras-type identities in non-symmetric problems, various quasi-orthogonality results have been developed; see [MN05; CN12; FFP14; BHP17]. We recall below the relaxed form (A4) from [Fei22], shown to hold *a priori* for uniformly inf-sup stable problems and, in particular, for the present Lax–Milgram setting.

Proposition 2. *There exist constants $C_{\text{orth}} > 0$ and $0 < \delta \leq 1$ such that, for any sequence $\mathcal{X}_\ell \subseteq \mathcal{X}_{\ell+1} \subseteq H_0^1(\Omega)$ of nested finite-dimensional subspaces, the exact discrete solutions $u_\ell^* \in \mathcal{X}_\ell$ to problem (7) satisfy, for all $\ell, N \in \mathbb{N}_0$,*

(A4) **Quasi-orthogonality:** $\sum_{\ell'=\ell}^{\ell+N} \|u_{\ell'+1}^* - u_{\ell'}^*\|^2 \leq C_{\text{orth}}(N+1)^{1-\delta} \|u^* - u_\ell^*\|^2.$

The constants C_{orth} and δ depend only on C_{bnd} and C_{ell} from (4).

3. DISCRETE ITERATIVE SMOOTHERS

3.1. Uniform stability and contraction. A smoother for the discrete variational problem (7) is represented by an iteration operator $\Psi_H: \mathcal{X}_H \rightarrow \mathcal{X}_H$. We consider the following two mesh-size-independent properties of such operators.

- (US) **Uniform stability:** There exists a constant $C_{\text{alg}} > 0$, independent of $\mathcal{T}_H \in \mathbb{T}$, such that, for all $v_H \in \mathcal{X}_H$, it holds that $\|u_H^* - \Psi_H(v_H)\| \leq C_{\text{alg}} \|u_H^* - v_H\|$.
- (UC) **Uniform contraction:** There exists a constant $0 < q_{\text{alg}} < 1$, independent of $\mathcal{T}_H \in \mathbb{T}$, such that (US) holds with $C_{\text{alg}} := q_{\text{alg}} < 1$.

3.2. Uniformly stable smoothers for symmetric PDEs. If the PDE (2) is symmetric, classic iterative methods for solving (7) contract the error in the energy norm, i.e., letting $\Psi_H: \mathcal{X}_H \rightarrow \mathcal{X}_H$ denote the iteration operator, there exists a contraction factor $0 < q_H < 1$, possibly depending on $\mathcal{T}_H \in \mathbb{T}$, such that

$$\|u_H^* - \Psi_H(v_H)\| \leq q_H \|u_H^* - v_H\| \quad \text{for all } v_H \in \mathcal{X}_H. \quad (10)$$

Although such Ψ_H are not uniformly contractive (UC) in general, contraction (10) immediately implies stability (US) with $C_{\text{alg}} = 1$. The mesh-dependent contraction (10) holds for essentially all classical smoothers; see the examples given below:

- *Richardson iteration* for sufficiently small damping [Hac16, Section 3.5.1].
- *Damped Jacobi iteration* for sufficiently small damping [Hac16, Theorem 6.11].
- *Gauss–Seidel iteration* [Hac16, Theorem 3.39].
- *Conjugate gradient method (CG)* [GV13, Theorem 11.3.3].
- *Preconditioned CG (PCG)* with an SPD preconditioner [GV13, Section 11.5.2], such as incomplete Cholesky preconditioners, provided the factorization terminates successfully, or block Jacobi preconditioners.

3.3. Uniformly stable smoothers for non-symmetric PDEs. To obtain uniformly stable (US) smoothers for non-symmetric problems, we symmetrize (7) and apply a stable smoother to the resulting symmetric system. Following [BIM⁺24], we use a single Zarantonello step [Zar60] for symmetrization. For $\delta > 0$, the Zarantonello operator $\mathcal{Z}_H^\delta: \mathcal{X}_H \rightarrow \mathcal{X}_H$ maps $v_H \in \mathcal{X}_H$ to the unique solution $\mathcal{Z}_H^\delta v_H \in \mathcal{X}_H$ of

$$a(\mathcal{Z}_H^\delta v_H, w_H) = a(v_H, w_H) + \delta [F(w_H) - b(v_H, w_H)] \quad \text{for all } w_H \in \mathcal{X}_H. \quad (11)$$

As $a(\cdot, \cdot)$ is an equivalent scalar product on $H_0^1(\Omega)$, the Riesz theorem ensures that \mathcal{Z}_H^δ is well-defined. The proof of [Zei90, Theorem 25.B], applied to \mathcal{X}_H endowed with $a(\cdot, \cdot)$, shows that \mathcal{Z}_H^δ is Lipschitz continuous in the energy norm, i.e., for all $v_H, w_H \in \mathcal{X}_H$,

$$\|\mathcal{Z}_H^\delta v_H - \mathcal{Z}_H^\delta w_H\| \leq C[\delta] \|v_H - w_H\| \quad \text{with} \quad C[\delta] = [1 - \delta(2 - \delta C_{\text{bnd}}^2/C_{\text{ell}}^2)]^{1/2}, \quad (12)$$

where $C_{\text{ell}}, C_{\text{bnd}}$ are the constants from (4). While $C[\delta] \geq 0$ for any choice of δ , we note that even $0 < C[\delta] < 1$ for $0 < \delta < 2C_{\text{ell}}^2/C_{\text{bnd}}^2$.

Adapting the reasoning from [BIM⁺24, Section 2], the next result shows that applying a uniformly stable smoother to (11) yields a uniformly stable smoother for the original non-symmetric system (7). The proof is provided in [Appendix A](#).

Proposition 3 (uniform stability of inexact Zarantonello symmetrization). *Let $\delta > 0$ and let $J \in \mathbb{N}_0$ be a number of smoother iterations. For every $\mathcal{T}_H \in \mathbb{T}$ and $v_H \in \mathcal{X}_H$, let $\Theta_H(v_H): \mathcal{X}_H \rightarrow \mathcal{X}_H$ be the iteration operator of a smoother for the symmetric problem (11), assumed to be uniformly stable in the sense that there exists a constant $C_{\text{alg}} > 0$, independent of the mesh size of \mathcal{T}_H and v_H , such that*

$$\|\mathcal{Z}_H^\delta v_H - \Theta_H(v_H)(w_H)\| \leq C_{\text{alg}} \|\mathcal{Z}_H^\delta v_H - w_H\| \quad \text{for all } w_H \in \mathcal{X}_H. \quad (13)$$

Then, the operator $\Psi_H: \mathcal{X}_H \rightarrow \mathcal{X}_H$ defined by $\Psi_H(v_H) := (\Theta_H(v_H))^J(v_H)$ is a uniformly stable **(US)** smoother for the non-symmetric system (7), i.e.,

$$\|u_H^* - \Psi_H(v_H)\| \leq [C[\delta] + C_{\text{alg}}^J(C[\delta] + 1)] \|u_H^* - v_H\| \quad \text{for all } v_H \in \mathcal{X}_H, \quad (14)$$

where $C[\delta]$ is the constant from (12). Moreover, provided that $\delta < 2C_{\text{ell}}^2/C_{\text{bnd}}^2$, there exists $J_0 \in \mathbb{N}$ such that Ψ_H is uniformly contractive **(UC)** for $J \geq J_0$.

4. SMOOTHED AFEM ALGORITHM

The S-AFEM loop in [Figure 2](#) distinguishes two types of refinement levels in the mesh hierarchy: *solve levels* and *intermediate levels*. Solve levels correspond to **SOLVE**, while intermediate levels correspond to **SMOOTH**. The spacing between two consecutive solve levels is determined by a fixed period $L \in \mathbb{N}$, so that the set of solve levels is given by $L \cdot \mathbb{N}_0 := \{\ell \in \mathbb{N}_0 \mid \ell = jL \text{ for some } j \in \mathbb{N}_0\}$. Two (generally different) iterative methods are employed. On solve levels, a uniformly contractive **(UC)** solver $\Phi_H: \mathcal{X}_H \rightarrow \mathcal{X}_H$ is applied and stopped according to a criterion balancing algebraic and discretization errors; see [BJR95; CS07; GHP21]. For symmetric problems, examples include the *hp*-robust geometric multigrid method from [IMPS24]. For non-symmetric problems, one may apply a uniformly contractive solver to the Zarantonello symmetrized problem (11), with [Proposition 3](#) guaranteeing **(UC)** for suitable parameter choices. On intermediate levels, a uniformly stable **(US)** smoother $\Psi_H: \mathcal{X}_H \rightarrow \mathcal{X}_H$ performs exactly $K \in \mathbb{N}$ iterations. In addition to standard Dörfler marking, a cardinality control step limits the number of marked elements on the intermediate levels. [Algorithm A](#) below formalizes this procedure.

Algorithm A (S-AFEM). *Given an initial mesh \mathcal{T}_0 , a number of smoothing steps $K \in \mathbb{N}_0$, a period $L \in \mathbb{N}$, adaptivity parameters $0 < \theta \leq 1, C_{\text{mark}}, C_{\text{card}} \geq 1$, a stopping parameter $\lambda > 0$, and an initial guess $u_0^0 \in \mathcal{X}_0$, iterate the following steps for $\ell = 0, 1, 2, \dots$:*

(I) **Case 1:** If $\ell \in L \cdot \mathbb{N}_0$, proceed with **SOLVE** & **ESTIMATE**:

For all $k = 1, 2, 3, \dots$, repeat the following steps (a)–(b) until

$$\|u_\ell^k - u_\ell^{k-1}\| \leq \lambda \eta_\ell(u_\ell^k). \quad (15)$$

- (a) Compute $u_\ell^k := \Phi_\ell(u_\ell^{k-1})$ with one step of the iterative solver.
- (b) Compute refinement indicator $\eta_\ell(T, u_\ell^k)$ for all $T \in \mathcal{T}_\ell$.

Upon termination of the preceding k -loop, define $\underline{k}[\ell] := k$.

(II) **Case 2:** If $\ell \notin L \cdot \mathbb{N}_0$, proceed with:

SMOOTH: For all $k = 1, \dots, K$, compute $u_\ell^k := \Psi_\ell(u_\ell^{k-1})$. Set $\underline{k}[\ell] := K$.

ESTIMATE: Compute refinement indicator $\eta_\ell(T, u_\ell^{\underline{k}[\ell]})$ for all $T \in \mathcal{T}_\ell$.

(III) **MARK:** Determine a set $\widetilde{\mathcal{M}}_\ell \subseteq \mathcal{T}_\ell$ with up to the factor C_{mark} minimal cardinality satisfying the Dörfler marking criterion $\theta \eta_\ell(u_\ell^{\underline{k}[\ell]})^2 \leq \eta_\ell(\widetilde{\mathcal{M}}_\ell, u_\ell^{\underline{k}[\ell]})^2$.

(IV) **MARK (CARDINALITY CONTROL):** Select a subset $\mathcal{M}_\ell \subseteq \widetilde{\mathcal{M}}_\ell$ such that

$$\mathcal{M}_\ell = \widetilde{\mathcal{M}}_\ell \text{ if } \ell \in L \cdot \mathbb{N}_0, \quad \text{and} \quad \#\mathcal{M}_\ell \leq C_{\text{card}} \#\mathcal{M}_{\ell-1} \text{ otherwise.} \quad (16)$$

(V) **REFINE**: Generate $\mathcal{T}_{\ell+1} := \text{refine}(\mathcal{T}_\ell, \mathcal{M}_\ell)$ and set $u_{\ell+1}^0 := u_\ell^{k[\ell]}$.

Remark 4. *Algorithm A* is a slight modification of the *S-AFEM* algorithm from [MGH21], formulated as a single loop with fixed period L . Moreover, *Algorithm A* introduces a novel cardinality-control step *Algorithm A(IV)* that modifies the preliminary Dörfler set $\widetilde{\mathcal{M}}_\ell$ from *Algorithm A(III)* to a final marking set \mathcal{M}_ℓ enforcing two key properties: First, on solve levels $\ell \in L \cdot \mathbb{N}_0$, no modification occurs, i.e., $\mathcal{M}_\ell = \widetilde{\mathcal{M}}_\ell$, so the Dörfler criterion remains valid. Second, on intermediate levels $\ell \in \mathbb{N}_0 \setminus L \cdot \mathbb{N}_0$, the cardinality $\#\mathcal{M}_\ell$ is bounded (up to C_{card}) by $\#\mathcal{M}_{\ell-1}$. Any subset $\mathcal{M}_\ell \subseteq \widetilde{\mathcal{M}}_\ell$ within this bound is admissible, including the extreme choice $\mathcal{M}_\ell = \emptyset$ on all intermediate levels. Evidently, a larger value of C_{card} allows $\mathcal{M}_\ell = \widetilde{\mathcal{M}}_\ell$ more often.

Remark 5. For $L = 1$, (II) and (IV) are void, so every mesh level employs a uniformly contractive solver (UC) with stopping criterion (15). Hence, *Algorithm A* reduces to the scheme of [GHP21; BFM⁺25], where full *R*-linear convergence and quasi-optimal complexity were established. For $L \geq 2$, uniformly contractive solvers are required only on the solve levels, while intermediate levels apply a fixed number of iterations of a uniformly stable smoother (US). Thus, *Algorithm A* significantly relaxes the algebraic requirements of [GHP21; BFM⁺25] while preserving the same convergence guarantees.

As is standard in adaptive algorithms with inexact solutions (see, e.g., [BFM⁺25]), we introduce the index set $\mathcal{Q} := \{(\ell, k) \in \mathbb{N}_0^2 \mid u_\ell^k \in \mathcal{X}_\ell\}$ defined in *Algorithm A* equipped with the partial order $(\ell', k') \leq (\ell, k)$ if $u_{\ell'}^{k'}$ is defined not later than u_ℓ^k in *Algorithm A*. For $(\ell, k) \in \mathcal{Q}$, define the total step counter by $|\ell, k| := \#\{(\ell', k') \in \mathcal{Q} \mid (\ell', k') < (\ell, k)\}$, which yields an order-preserving bijection $|\cdot|: \mathcal{Q} \rightarrow \mathbb{N}_0$. We write $\underline{k} = \underline{k}[\ell]$ when the index ℓ is clear from the context, e.g., u_ℓ^k instead of $u_\ell^{k[\ell]}$. Define the stopping index of the mesh-refinement loop by $\underline{\ell} := \sup\{\ell \in \mathbb{N}_0 \mid (\ell, 0) \in \mathcal{Q}\} \in \mathbb{N}_0 \cup \{+\infty\}$. Typically, $\underline{\ell} = +\infty$, i.e., the stopping criterion (15) is satisfied after finitely many solver steps $\underline{k}[\ell] \in \mathbb{N}$ on each solve level $\ell \in L \cdot \mathbb{N}_0$. In the case $\underline{\ell} < +\infty$, the solver $\Phi_{\underline{\ell}}$ fails to terminate on $\mathcal{T}_{\underline{\ell}}$ and we set $\underline{k}[\underline{\ell}] := +\infty$, which can only occur for $\underline{\ell} \in L \cdot \mathbb{N}_0$. To cover this case, define the set of reached solve levels by $\underline{\mathcal{S}} := \{\ell \in L \cdot \mathbb{N}_0 \mid (\ell, 0) \in \mathcal{Q}\}$ and the subset $\mathcal{S} := \underline{\mathcal{S}} \setminus \{\underline{\ell}\}$ where the solver terminates. If $\underline{\ell} = +\infty$, then $\underline{\mathcal{S}} = \mathcal{S} = L \cdot \mathbb{N}_0$. In either case, $u_\ell^{k[\ell]} \in \mathcal{X}_\ell$ is well-defined for all $\ell \in \mathcal{S}$. Similarly, define the set of reached intermediate levels by $\mathcal{I} := \{\ell \in \mathbb{N}_0 \setminus L \cdot \mathbb{N}_0 \mid (\ell, 0) \in \mathcal{Q}\}$.

5. FULL R-LINEAR CONVERGENCE

This section establishes two results asserting full *R*-linear convergence of *Algorithm A*. The first result, *Theorem 6*, establishes *unconditional* full *R*-linear convergence for any choice of input parameters, provided the smoother is stable (US) with $C_{\text{alg}} \leq 1$. This mild assumption is satisfied by classical smoothers (cf. *subsection 3.2*) and even by the identity operator. The second result, *Theorem 12*, uses a perturbation argument to show that the restriction $C_{\text{alg}} \leq 1$ can even be removed when the stopping parameter $\lambda > 0$ is chosen sufficiently small.

Theorem 6 (unconditional full R-linear convergence). *Assume that the solver Φ_ℓ is uniformly contractive (UC) and that the smoother Ψ_ℓ is uniformly stable (US) with $C_{\text{alg}} \leq 1$. Let $K, L \in \mathbb{N}, C_{\text{mark}}, C_{\text{card}} \geq 1, \lambda > 0$, $u_0^0 \in \mathcal{X}_0$, and $0 < \theta \leq 1$ be arbitrary. Then, *Algorithm A* guarantees full *R*-linear convergence of the quasi-error*

$$\mathsf{H}_\ell^k := \|u_\ell^* - u_\ell^k\| + \eta_\ell(u_\ell^*), \quad (17)$$

i.e., there exist constants $C_{\text{lin}} > 0$ and $0 < q_{\text{lin}} < 1$ such that

$$\mathsf{H}_\ell^k \leq C_{\text{lin}} q_{\text{lin}}^{|\ell, k| - |\ell', k'|} \mathsf{H}_{\ell'}^{k'} \quad \text{for all } (\ell', k'), (\ell, k) \in \mathcal{Q} \text{ with } |\ell', k'| \leq |\ell, k|. \quad (18)$$

The constants $C_{\text{lin}}, q_{\text{lin}}$ depend only on K, L, λ, θ , and the constants in (A1)–(A4) and (QM). Specifically, the constants $C_{\text{lin}}, q_{\text{lin}}$ grow at most linearly in K and at most exponentially in L (the precise bounds are detailed in Step 5 of the proof).

Remark 7. *R-linear convergence (18) implies convergence of Algorithm A via*

$$\|u^* - u_\ell^k\| \leq \|u^* - u_\ell^*\| + \|u_\ell^* - u_\ell^k\| \stackrel{(A3)}{\lesssim} H_\ell^k \stackrel{(18)}{\leq} C_{\text{lin}} q_{\text{lin}}^{|\ell,k|} H_0^0 \xrightarrow{|\ell,k| \rightarrow \infty} 0.$$

In particular, if $\underline{\ell} < +\infty$, then $\eta_{\underline{\ell}}(u_\ell^*) \leq H_\ell^k \rightarrow 0$ as $k \rightarrow \infty$ implies $\eta_{\underline{\ell}}(u_\ell^*) = 0$ and hence $u^* = u_\ell^*$ by reliability (A3), i.e., the case $\underline{\ell} < +\infty$ can only occur if u^* is discrete.

Remark 8. *Theorem 6 remains valid in the degenerate case $C_{\text{card}} = +\infty$, in which cardinality control (16) is void and $\mathcal{M}_\ell = \widetilde{\mathcal{M}}_\ell$ is admissible on all mesh levels.*

The proof of Theorem 6 is based on the characterization of full R-linear convergence (18) from [BFM⁺25, Lemma 2], showing that (18) is equivalent to *tail summability*

$$\sum_{\substack{(\ell',k') \in \mathcal{Q} \\ |\ell',k'| > |\ell,k|}} H_{\ell'}^{k'} \leq C'_{\text{lin}} H_\ell^k \quad \text{for all } (\ell, k) \in \mathcal{Q} \quad (19)$$

for a certain constant $C'_{\text{lin}} > 0$. The proof of (19) relies on the following two lemmas. The first refines [BFM⁺25, Lemma 1] by omitting one of its assumptions.

Lemma 9 (tail summability criterion). *Let $(a_j)_{j \in \mathbb{N}_0}$ and $(b_j)_{j \in \mathbb{N}_0}$ be sequences in $\mathbb{R}_{\geq 0}$. Suppose there exist constants $0 < q < 1$, $0 < \delta \leq 1$, and $C > 0$ such that*

$$a_{j+1} \leq qa_j + b_j \quad \text{and} \quad \sum_{j'=j}^{j+N} b_{j'}^2 \leq C(N+1)^{1-\delta} a_j^2 \quad \text{for all } j, N \in \mathbb{N}_0. \quad (20)$$

Then, the sequence $(a_j)_{j \in \mathbb{N}_0}$ is tail summable, i.e., there exists $\tilde{C} > 0$ such that

$$\sum_{j'=j+1}^{\infty} a_{j'} \leq \tilde{C} a_j \quad \text{for all } j \in \mathbb{N}_0. \quad (21)$$

The optimal constant \tilde{C} in (21) is bounded in the following sense. Given $0 < \varepsilon < q^{-2} - 1$, define, for all $N \in \mathbb{N}_0$,

$$M(N) := \frac{1 + (1 + \varepsilon^{-1})CN^{1-\delta}}{1 - (1 + \varepsilon)q^2} \prod_{R=1}^N \frac{(1 + \varepsilon)q^2 + (1 + \varepsilon^{-1})CR^{1-\delta}}{1 + (1 + \varepsilon^{-1})CR^{1-\delta}} > 0. \quad (22)$$

Then, there exists $N_0 \in \mathbb{N}$ such that $M(N_0) < 1$. For any such choice of N_0 and ε ,

$$\tilde{C} \leq \frac{M(N_0)^{(1-N_0)/(2N_0)}}{1 - M(N_0)^{1/(2N_0)}} \max_{R=0, \dots, N_0-1} M(R)^{1/2}. \quad (23)$$

Proof. Let $0 < \varepsilon < q^{-2} - 1$. Arguing as in the proof of [BFM⁺25, Lemma 1], the perturbed contraction and the summability from (20) imply that, for $M(N)$ from (22),

$$a_{j+N}^2 \leq M(N) a_j^2 \quad \text{for all } j, N \in \mathbb{N}_0 \quad \text{and} \quad M(N) \rightarrow 0 \text{ as } N \rightarrow +\infty. \quad (24)$$

Choose $N_0 \in \mathbb{N}$ such that $M(N_0) < 1$. For arbitrary $N \in \mathbb{N}_0$, write $N = mN_0 + r$ with $m, r \in \mathbb{N}_0$ and $r < N_0$. Repeated application of (24) gives

$$\begin{aligned} a_{j+N}^2 &= a_{j+mN_0+r}^2 \stackrel{(24)}{\leq} M(N_0)^m a_{j+r}^2 \stackrel{(24)}{\leq} \left(\max_{R=0, \dots, N_0-1} M(R) \right) M(N_0)^m a_j^2 \\ &\leq \left(\max_{R=0, \dots, N_0-1} M(R) \right) M(N_0)^{N/N_0-1} a_j^2. \end{aligned} \quad (25)$$

Taking square roots in (25) establishes R-linear convergence of $(a_j)_{j \in \mathbb{N}_0}$ with constants $\tilde{C}_{\text{lin}} := \max_{R=0, \dots, N_0-1} M(R)^{1/2} M(N_0)^{-1/2} > 0$ and $\tilde{q}_{\text{lin}} := M(N_0)^{1/(2N_0)} < 1$. Hence, by [BFM⁺25, Lemma 2], tail summability (21) holds with $\tilde{C} \leq \tilde{C}_{\text{lin}} \tilde{q}_{\text{lin}} / (1 - \tilde{q}_{\text{lin}})$. Inserting the definition of $M(N)$ from (22) thus yields the explicit bound in (23). \square

The second lemma delivers the novel key idea by establishing tail summability of H_ℓ^k along the solve levels via Dörfler marking, solver contraction (UC), and Lemma 9.

Lemma 10 (tail summability along solve levels). *Under the assumptions of Theorem 6, the quasi-error H_ℓ^k of the final iterates u_ℓ^k generated by Algorithm A is tail summable on the solve levels, i.e., there exists a constant $C_{\text{tail}} > 0$ such that*

$$\sum_{\ell' \in \mathcal{S}, \ell' > \ell} \mathsf{H}_{\ell'}^k \leq C_{\text{tail}} \mathsf{H}_\ell^k \quad \text{for all } \ell \in \mathcal{S}. \quad (26)$$

The constant C_{tail} depends only on $L, \theta, q_{\text{alg}}$, and the constants in (A1)–(A4).

Proof. The proof is split into four steps.

Step 1. Let $\ell \in \mathcal{S}$ be a solve level with $\ell + L \in \mathcal{S}$. Due to (A1)–(A2), we have

$$\begin{aligned} \eta_{\ell+L}(u_\ell^k)^2 &\leq \eta_\ell(\mathcal{T}_{\ell+L} \cap \mathcal{T}_\ell, u_\ell^k) + q_{\text{red}}^2 \eta_\ell(\mathcal{T}_\ell \setminus \mathcal{T}_{\ell+L}, u_\ell^k) \\ &= \eta_\ell(u_\ell^k)^2 - (1 - q_{\text{red}}^2) \eta_\ell(\mathcal{T}_\ell \setminus \mathcal{T}_{\ell+L}, u_\ell^k). \end{aligned}$$

By (III)–(IV), \mathcal{M}_ℓ satisfies the Dörfler criterion. Since $\mathcal{M}_\ell \subseteq \mathcal{T}_\ell \setminus \mathcal{T}_{\ell+L}$, it follows that

$$\theta \eta_\ell(u_\ell^k)^2 \leq \eta_\ell(\mathcal{M}_\ell, u_\ell^k)^2 \leq \eta_\ell(\mathcal{T}_\ell \setminus \mathcal{T}_{\ell+L}, u_\ell^k)^2.$$

The combination of the previous two displayed formulas leads to

$$\eta_{\ell+L}(u_\ell^k) \leq q_\theta \eta_\ell(u_\ell^k) \quad \text{with} \quad 0 < q_\theta := [1 - (1 - q_{\text{red}}^2)\theta]^{1/2} < 1. \quad (27)$$

From (27) together with stability (A1), we obtain

$$\eta_{\ell+L}(u_{\ell+L}^k) \leq q_\theta \eta_\ell(u_\ell^k) + C_{\text{stab}} \|u_{\ell+L}^k - u_\ell^k\|. \quad (28)$$

For all $\ell \in \mathcal{S}$, define

$$\sigma_\ell := \sum_{\ell'=\ell}^{\ell+L-1} \|u_{\ell'+1}^* - u_{\ell'}^*\|. \quad (29)$$

Since $(\ell + L - 1, 0) \in \mathcal{Q}$ for all $\ell \in \mathcal{S}$, σ_ℓ is well-defined. There holds

$$\|u_{\ell+L}^k - u_\ell^k\| \leq \|u_{\ell+L}^* - u_{\ell+L}^k\| + \|u_{\ell+L}^* - u_\ell^k\| \leq \|u_{\ell+L}^* - u_{\ell+L}^k\| + \|u_\ell^* - u_\ell^k\| + \sigma_\ell. \quad (30)$$

The combination of (28) and (30) shows that, for all $\ell \in \mathcal{S}$ with $\ell + L \in \mathcal{S}$,

$$\eta_{\ell+L}(u_{\ell+L}^k) \leq q_\theta \eta_\ell(u_\ell^k) + C_{\text{stab}} (\|u_{\ell+L}^* - u_{\ell+L}^k\| + \|u_\ell^* - u_\ell^k\| + \sigma_\ell). \quad (31)$$

Step 2. Let $\ell \in \mathcal{S}$ and $0 < r < L$. From $\underline{k}[\ell + r] = K$, nested iteration $u_{\ell+r}^0 = u_{\ell+r-1}^k$, and the stability (US) with $C_{\text{alg}} \leq 1$, it follows that

$$\|u_{\ell+r}^* - u_{\ell+r}^k\| \stackrel{(US)}{\leq} C_{\text{alg}}^K \|u_{\ell+r}^* - u_{\ell+r}^0\| \leq \|u_{\ell+r-1}^* - u_{\ell+r-1}^k\| + \|u_{\ell+r}^* - u_{\ell+r-1}^*\|.$$

The successive application of this argument and including the trivial case $r = 0$ verifies

$$\|u_{\ell+r}^* - u_{\ell+r}^k\| \leq \|u_\ell^* - u_\ell^k\| + \sum_{\ell'=\ell}^{\ell+r-1} \|u_{\ell'+1}^* - u_{\ell'}^*\| \quad \text{for all } \ell \in \mathcal{S}, 0 \leq r < L. \quad (32)$$

Step 3. Let $\ell \in \mathcal{S}$ with $\ell + L \in \mathcal{S}$. The nested iteration $u_{\ell+L}^0 = u_{\ell+L-1}^k$, the solver contraction (UC), the bound $\underline{k}[\ell+L] \geq 1$, and (32) with $r = L - 1$ show that

$$\begin{aligned} \|u_{\ell+L}^* - u_{\ell+L}^k\| &\stackrel{(UC)}{\leq} q_{\text{alg}}^{k[\ell+L]} \|u_{\ell+L}^* - u_{\ell+L}^0\| \leq q_{\text{alg}} \|u_{\ell+L}^* - u_{\ell+L-1}^k\| \\ &\leq q_{\text{alg}} (\|u_{\ell+L-1}^* - u_{\ell+L-1}^k\| + \|u_{\ell+L}^* - u_{\ell+L-1}^*\|) \\ &\stackrel{(32)}{\leq} q_{\text{alg}} \left(\|u_\ell^* - u_\ell^k\| + \sum_{\ell'=\ell}^{\ell+L-1} \|u_{\ell'+1}^* - u_{\ell'}^*\| \right) \stackrel{(29)}{=} q_{\text{alg}} (\|u_\ell^* - u_\ell^k\| + \sigma_\ell). \end{aligned} \quad (33)$$

Step 4. For $j \in \mathbb{N}_0$ with $jL < \underline{\ell}$, define $C_\gamma := \gamma C_{\text{stab}}$, $a_j := \|u_{jL}^* - u_{jL}^k\| + \gamma \eta_{jL}(u_{jL}^k)$, and $b_j := q\sigma_{jL}$, where $0 < \gamma \leq 1$ is chosen so that $q := \max\{q_{\text{alg}} + C_\gamma(1 + q_{\text{alg}}), q_\theta\} < 1$. For $j \in \mathbb{N}_0$ with $(j+1)L < \underline{\ell}$, (31) and (33) with $\ell = jL$ give

$$\begin{aligned} a_{j+1} &\stackrel{(31)}{\leq} (1 + C_\gamma) \|u_{jL+L}^* - u_{jL+L}^k\| + \gamma q_\theta \eta_{jL}(u_{jL}^k) + C_\gamma (\|u_{jL}^* - u_{jL}^k\| + \sigma_{jL}) \\ &\stackrel{(33)}{\leq} [q_{\text{alg}} + C_\gamma(1 + q_{\text{alg}})] (\|u_{jL}^* - u_{jL}^k\| + \sigma_{jL}) + \gamma q_\theta \eta_{jL}(u_{jL}^k) \leq qa_j + b_j. \end{aligned} \quad (34)$$

Moreover, from stability (A1) and reliability (A3), it follows that

$$\|u^* - u_{jL}^*\| \stackrel{(A3)}{\lesssim} \eta_{jL}(u_{jL}^*) \stackrel{(A1)}{\lesssim} \eta_{jL}(u_{jL}^k) + \|u_{jL}^* - u_{jL}^k\| \simeq a_j. \quad (35)$$

Together with (A4), the previous estimate shows, for all $N \in \mathbb{N}_0$ with $(j+N)L < \underline{\ell}$,

$$\begin{aligned} \sum_{j'=j}^{j+N} \sigma_{j'L}^2 &\leq L \sum_{j'=j}^{j+N} \sum_{\ell'=j'L}^{j'L+L-1} \|u_{\ell'+1}^* - u_{\ell'}^*\|^2 = L \sum_{\ell'=jL}^{jL+(N+1)L-1} \|u_{\ell'+1}^* - u_{\ell'}^*\|^2 \\ &\stackrel{(A4)}{\lesssim} L((N+1)L)^{1-\delta} \|u^* - u_{jL}^*\|^2 \stackrel{(35)}{\lesssim} L^{2-\delta} (N+1)^{1-\delta} a_j^2, \end{aligned} \quad (36)$$

where the hidden constant depends only on $\theta, q_{\text{alg}}, \gamma$, and the constants in (A1)–(A4). By (34), (36), and $b_j \leq \sigma_{jL}$, $(a_j)_{j \in \mathbb{N}_0}$ and $(b_j)_{j \in \mathbb{N}_0}$ (extended by zero if $\underline{\ell} < +\infty$) satisfy the assumptions (20) of Lemma 9. Hence, $(a_j)_{j \in \mathbb{N}_0}$ is tail summable, i.e.,

$$\sum_{j'=j+1}^{\underline{\ell}/L-1} a_{j'} \stackrel{(21)}{\lesssim} a_j \quad \text{for all } j \in \mathbb{N}_0 \text{ with } jL < \underline{\ell}. \quad (37)$$

Finally, since, for all $j \in \mathbb{N}_0$ with $jL < \underline{\ell}$,

$$\mathsf{H}_{jL}^k \stackrel{(17)}{=} \|u_{jL}^* - u_{jL}^k\| + \eta_{jL}(u_{jL}^*) \stackrel{(A1)}{\simeq} \|u_{jL}^* - u_{jL}^k\| + \eta_{jL}(u_{jL}^k) \simeq a_j,$$

and every $\ell \in \mathcal{S}$ can be written as $\ell = jL$ for some $j \in \mathbb{N}_0$ with $jL < \underline{\ell}$, the desired tail summability (26) follows from (37). This concludes the proof. \square

The central idea in proving Theorem 6 is that extending (26) to tail summability of the full sequence requires only (US) on intermediate and (UC) on solve levels.

Proof of Theorem 6. The proof is divided into five steps.

Step 1 (monotonicity in k). Let $(\ell, k), (\ell, k') \in \mathcal{Q}$ with $k \leq k'$. The solver contraction (UC) and the smoother stability (US) with $C_{\text{alg}} \leq 1$ yield

$$\mathsf{H}_\ell^{k'} \stackrel{(17)}{=} \|u_\ell^* - u_\ell^{k'}\| + \eta_\ell(u_\ell^*) \leq \max\{q_{\text{alg}}, C_{\text{alg}}\}^{k'-k} \|u_\ell^* - u_\ell^k\| + \eta_\ell(u_\ell^*) \leq \mathsf{H}_\ell^k.$$

Hence, it holds

$$\mathsf{H}_\ell^{k'} \leq \mathsf{H}_\ell^k \quad \text{for all } (\ell, k), (\ell, k') \in \mathcal{Q} \text{ with } k \leq k'. \quad (38)$$

Step 2 (tail summability in k). For intermediate levels $\ell \in \mathcal{I}$, tail summability in k follows immediately from (38) and $\underline{k}[\ell] = K$ via

$$\sum_{k'=k+1}^{\underline{k}[\ell]} \mathsf{H}_\ell^{k'} \stackrel{(38)}{\leq} \sum_{k'=k+1}^{\underline{k}[\ell]} \mathsf{H}_\ell^k \leq K \mathsf{H}_\ell^k \quad \text{for all } \ell \in \mathcal{I} \text{ and all } k < \underline{k}[\ell] = K. \quad (39)$$

Next, consider an arbitrary solve level $\ell \in \underline{\mathcal{S}}$. Let $0 \leq k < k' < \underline{k}[\ell]$. The failure of the stopping criterion (15) and uniform contraction (UC) of the iterative solver yield

$$\lambda \eta_\ell(u_\ell^{k'}) \stackrel{(15)}{<} \|u_\ell^{k'} - u_\ell^{k'-1}\| \stackrel{(\text{UC})}{\leq} q_{\text{alg}}^{-1} (1 + q_{\text{alg}}) q_{\text{alg}}^{k'-k} \|u_\ell^* - u_\ell^k\|. \quad (40)$$

Set $C_1 := 1 + C_{\text{stab}} + \lambda^{-1} q_{\text{alg}}^{-1} (1 + q_{\text{alg}})$. Together with stability (A1) and $\|u_\ell^* - u_\ell^k\| \leq \mathsf{H}_\ell^k$, this shows that, for all $0 \leq k < k' < \underline{k}[\ell]$,

$$\begin{aligned} \mathsf{H}_\ell^{k'} &\stackrel{(\text{A1})}{\leq} (1 + C_{\text{stab}}) \|u_\ell^* - u_\ell^k\| + \eta_\ell(u_\ell^{k'}) \\ &\stackrel{(\text{UC})}{\leq} (1 + C_{\text{stab}}) q_{\text{alg}}^{k'-k} \|u_\ell^* - u_\ell^k\| + \eta_\ell(u_\ell^{k'}) \stackrel{(40)}{\leq} C_1 q_{\text{alg}}^{k'-k} \mathsf{H}_\ell^k. \end{aligned} \quad (41)$$

The estimate (41) and the geometric series prove, for all $\ell \in \underline{\mathcal{S}}$ and all $k < \underline{k}[\ell]$,

$$\begin{aligned} \sum_{k'=k+1}^{\underline{k}[\ell]} \mathsf{H}_\ell^{k'} &= \mathsf{H}_\ell^k + \sum_{k'=k+1}^{\underline{k}[\ell]-1} \mathsf{H}_\ell^{k'} \stackrel{(41)}{\leq} \mathsf{H}_\ell^k + C_1 \mathsf{H}_\ell^k \sum_{k'=k+1}^{\underline{k}[\ell]-1} q_{\text{alg}}^{k'-k} \\ &\stackrel{(38)}{\leq} [1 + C_1(1 - q_{\text{alg}})^{-1}] \mathsf{H}_\ell^k. \end{aligned} \quad (42)$$

Set $C_2 := \max\{K, 1 + C_1(1 - q_{\text{alg}})^{-1}\}$. Then, combining (39) and (42), we conclude

$$\sum_{k'=k+1}^{\underline{k}[\ell]} \mathsf{H}_\ell^{k'} \leq C_2 \mathsf{H}_\ell^k \quad \text{for all } (\ell, k) \in \mathcal{Q} \text{ with } k < \underline{k}[\ell]. \quad (43)$$

Step 3 (stability under mesh refinement). By (QM) and $u_\ell^0 = u_{\ell-1}^k$, it holds

$$\begin{aligned} \mathsf{H}_\ell^0 &\stackrel{(\text{QM})}{\leq} C_{\text{mon}} [\|u_\ell^* - u_\ell^0\| + \eta_{\ell-1}(u_{\ell-1}^*)] \\ &\leq C_{\text{mon}} [\|u_\ell^* - u_{\ell-1}^*\| + \|u_{\ell-1}^* - u_\ell^0\| + \eta_{\ell-1}(u_{\ell-1}^*)] \stackrel{(17)}{=} C_{\text{mon}} [\|u_\ell^* - u_{\ell-1}^*\| + \mathsf{H}_{\ell-1}^k]. \end{aligned}$$

To bound $\|u_\ell^* - u_{\ell-1}^*\|$, we use reliability (A3) and quasi-monotonicity (QM) to deduce

$$\|u_\ell^* - u_{\ell-1}^*\| \stackrel{(\text{A3})}{\leq} C_{\text{rel}} [\eta_\ell(u_\ell^*) + \eta_{\ell-1}(u_{\ell-1}^*)] \stackrel{(\text{QM})}{\leq} C_{\text{rel}} (1 + C_{\text{mon}}) \eta_{\ell-1}(u_{\ell-1}^*).$$

For $C_3 := C_{\text{mon}}[C_{\text{rel}}(1 + C_{\text{mon}}) + 1]$, the previous two displayed formulas result in

$$\mathsf{H}_\ell^0 \leq C_3 \mathsf{H}_{\ell-1}^k. \quad (44)$$

Repeated application of (44) gives

$$\mathsf{H}_\ell^k \stackrel{(38)}{\leq} \mathsf{H}_\ell^0 \stackrel{(44)}{\leq} C_3^j \mathsf{H}_{\ell-j}^k \quad \text{for all } 0 \leq j \leq \ell < \underline{\ell}. \quad (45)$$

Step 4 (tail summability of H_ℓ^k in ℓ). Denote by $\text{mod}(\ell, L)$ the unique integer $0 \leq r < L$ such that $\ell - r \in L \cdot \mathbb{N}_0$. Let $\ell \in \mathbb{N}_0$ with $\ell < \underline{\ell}$ and let $\ell_0 \in L \cdot \mathbb{N}_0$ be the minimal index such

that $\ell_0 \geq \underline{\ell}$. In particular, $\ell_0 - \underline{\ell} \leq L - 1$. For the first case, suppose that $\ell_0 < \underline{\ell}$, which ensures that $\ell_0 \in \mathcal{S}$. Then, the tail sum decomposes as

$$\sum_{\ell'=\ell+1}^{\underline{\ell}-1} \mathsf{H}_{\ell'}^k = \sum_{\ell'=\ell+1}^{\ell_0} \mathsf{H}_{\ell'}^k + \sum_{\ell' \in \mathcal{S}, \ell_0 < \ell'} \mathsf{H}_{\ell'}^k + \sum_{\ell' \in \mathcal{I}, \ell_0 < \ell'} \mathsf{H}_{\ell'}^k. \quad (46)$$

To estimate the first sum in (46), we apply (45) and $C_3 \geq 1$ to deduce

$$\sum_{\ell'=\ell+1}^{\ell_0} \mathsf{H}_{\ell'}^k \stackrel{(45)}{\leq} \sum_{\ell'=\ell+1}^{\ell_0} C_3^{\ell'-\underline{\ell}} \mathsf{H}_{\underline{\ell}}^k = \frac{C_3^{\ell_0-\underline{\ell}+1} - C_3}{C_3 - 1} \mathsf{H}_{\underline{\ell}}^k \leq \frac{C_3^L - C_3}{C_3 - 1} \mathsf{H}_{\underline{\ell}}^k. \quad (47)$$

For the second sum in (46), we apply Lemma 10, (45), and $C_3 \geq 1$ to obtain

$$\sum_{\ell' \in \mathcal{S}, \ell_0 < \ell'} \mathsf{H}_{\ell'}^k \stackrel{(26)}{\leq} C_{\text{tail}} \mathsf{H}_{\ell_0}^k \stackrel{(45)}{\leq} C_{\text{tail}} C_3^{\ell_0-\underline{\ell}} \mathsf{H}_{\underline{\ell}}^k \leq C_{\text{tail}} C_3^{L-1} \mathsf{H}_{\underline{\ell}}^k. \quad (48)$$

To estimate the third sum in (46), note that there are exactly $L - 1$ intermediate levels between consecutive solve levels. Hence, Lemma 10 and (45) imply that

$$\begin{aligned} \sum_{\ell' \in \mathcal{I}, \ell_0 < \ell'} \mathsf{H}_{\ell'}^k &\stackrel{(45)}{\leq} \sum_{\ell' \in \mathcal{I}, \ell_0 < \ell'} C_3^{\text{mod}(\ell', L)} \mathsf{H}_{\ell'-\text{mod}(\ell', L)}^k \leq \sum_{\ell' \in \mathcal{S}, \ell_0 \leq \ell'} \sum_{j=1}^{L-1} C_3^j \mathsf{H}_{\ell'}^k \\ &\stackrel{(26)}{\leq} \sum_{j=1}^{L-1} C_3^j (1 + C_{\text{tail}}) \mathsf{H}_{\ell_0}^k \stackrel{(45)}{\leq} \sum_{j=1}^{L-1} C_3^j (1 + C_{\text{tail}}) C_3^{L-1} \mathsf{H}_{\underline{\ell}}^k. \end{aligned} \quad (49)$$

Using $\sum_{j=1}^{L-1} C_3^j = \frac{C_3^L - C_3}{C_3 - 1}$ and (47)–(49), we estimate (46) via

$$\sum_{\ell'=\ell+1}^{\underline{\ell}-1} \mathsf{H}_{\ell'}^k \leq \left(\frac{C_3^L - C_3}{C_3 - 1} + C_{\text{tail}} C_3^{L-1} + \frac{C_3^L - C_3}{C_3 - 1} (1 + C_{\text{tail}}) C_3^{L-1} \right) \mathsf{H}_{\underline{\ell}}^k =: C_4 \mathsf{H}_{\underline{\ell}}^k. \quad (50)$$

The remaining case $\ell_0 \geq \underline{\ell}$ can only occur if $\ell_0 = \underline{\ell} \in L \cdot \mathbb{N}_0$. Therefore, $\underline{\ell} - \ell \leq L - 1$, and thus the stability estimate (45) yields

$$\sum_{\ell'=\ell+1}^{\underline{\ell}-1} \mathsf{H}_{\ell'}^k \stackrel{(45)}{\leq} \sum_{\ell'=\ell+1}^{\underline{\ell}-1} C_3^{\ell'-\underline{\ell}} \mathsf{H}_{\underline{\ell}}^k = \frac{C_3^{\underline{\ell}-\ell} - C_3}{C_3 - 1} \mathsf{H}_{\underline{\ell}}^k \leq \frac{C_3^{L-1} - C_3}{C_3 - 1} \mathsf{H}_{\underline{\ell}}^k \leq C_4 \mathsf{H}_{\underline{\ell}}^k. \quad (51)$$

Overall, the combination of (50)–(51) shows that

$$\sum_{\ell'=\ell+1}^{\underline{\ell}-1} \mathsf{H}_{\ell'}^k \leq C_4 \mathsf{H}_{\underline{\ell}}^k \quad \text{for all } 0 \leq \ell < \underline{\ell}. \quad (52)$$

Step 5 (tail summability of H_{ℓ}^k in ℓ and k). For $C_5 := C_3(1 + C_4)$, it holds

$$\sum_{\ell'=\ell+1}^{\underline{\ell}} \mathsf{H}_{\ell'}^0 \stackrel{(44)}{\leq} C_3 \sum_{\ell'=\ell}^{\underline{\ell}-1} \mathsf{H}_{\ell'}^k \stackrel{(52)}{\leq} C_3(1 + C_4) \mathsf{H}_{\underline{\ell}}^k \stackrel{(38)}{\leq} C_5 \mathsf{H}_{\underline{\ell}}^k. \quad (53)$$

Set $C_6 := C_2(1 + 2C_5)$. From $C_2 \geq 1$, (43) and (53), we obtain

$$\begin{aligned} \sum_{\substack{(\ell', k') \in \mathcal{Q} \\ |\ell', k'| > |\ell, k|}} \mathsf{H}_{\ell'}^{k'} &= \sum_{k'=k+1}^{k[\ell]} \mathsf{H}_{\ell'}^{k'} + \sum_{\ell'=\ell+1}^{\underline{\ell}} \sum_{k'=0}^{k[\ell']} \mathsf{H}_{\ell'}^{k'} \stackrel{(43)}{\leq} C_2 \left(\mathsf{H}_{\ell}^k + 2 \sum_{\ell'=\ell+1}^{\underline{\ell}} \mathsf{H}_{\ell'}^0 \right) \stackrel{(53)}{\leq} C_6 \mathsf{H}_{\underline{\ell}}^k. \end{aligned}$$

By the preceding estimate, the sequence H_ℓ^k is tail summable with constant

$$\begin{aligned} C_6 = \max \left\{ K, 1 + \frac{1 + C_{\text{stab}} + \lambda^{-1} q_{\text{alg}}^{-1} (1 + q_{\text{alg}})}{1 - q_{\text{alg}}} \right\} \\ \times \left[1 + 2C_3 + \left(\frac{C_3^L - C_3}{C_3 - 1} (2C_3 + 2C_3^L + 2C_{\text{tail}}C_3^L) + 2C_{\text{tail}}C_3^L \right) \right], \end{aligned}$$

where $C_3 = C_{\text{mon}}[C_{\text{rel}}(1 + C_{\text{mon}}) + 1] > 1$ stems from (44). Thus, [BFM⁺25, Lemma 2] yields R-linear convergence (18) with constants $C_{\text{lin}} \leq C_6 + 1$ and $q_{\text{lin}} \leq (1 + C_6^{-1})^{-1}$. \square

For sufficiently small $\lambda > 0$, the stopping criterion (15) together with uniform contraction (UC) guarantees estimator equivalence $\eta_\ell(u_\ell^k) \simeq \eta_\ell(u_\ell^*)$ on the solve levels $\ell \in \mathcal{S}$. The following lemma, essentially from [GHP18, Lemma 4.9], states this precisely.

Lemma 11 (estimator equivalence). *Suppose that Φ_ℓ satisfies (UC). Define*

$$\lambda_{\text{opt}} := (1 - q_{\text{alg}})/(C_{\text{stab}}q_{\text{alg}}). \quad (54)$$

If $0 < \lambda < \lambda_{\text{opt}}$, then the final iterates $u_\ell^k \in \mathcal{X}_\ell$ generated by Algorithm A satisfy

$$(1 - \lambda\lambda_{\text{opt}}^{-1})\eta_\ell(u_\ell^k) \leq \eta_\ell(u_\ell^*) \leq (1 + \lambda\lambda_{\text{opt}}^{-1})\eta_\ell(u_\ell^k) \quad \text{for all } \ell \in \mathcal{S}. \quad (55)$$

\square

By a standard perturbation argument, the estimator equivalence (55) implies tail summability along solve levels (26) even for arbitrary $C_{\text{alg}} > 0$. The extension to the full sequence proceeds analogously to the proof of Theorem 6. Hence, for sufficiently small $\lambda > 0$, the restriction $C_{\text{alg}} \leq 1$ on the smoother in Theorem 6 may be dropped, leading to the following result. A proof is provided in Appendix A.

Theorem 12 (full R-linear convergence for arbitrary $C_{\text{alg}} > 0$). *Let the assumptions of Theorem 6 hold, except that the smoother Ψ_ℓ satisfies uniform stability (US) with an arbitrary constant $C_{\text{alg}} > 0$. Recall λ_{opt} from (54). If $0 < \lambda < \theta^{1/2}\lambda_{\text{opt}}$, then Algorithm A guarantees full R-linear convergence of the quasi-error H_ℓ^k from (17), i.e., there exist constants $C_{\text{lin}} > 0$ and $0 < q_{\text{lin}} < 1$ such that*

$$\mathsf{H}_\ell^k \leq C_{\text{lin}}q_{\text{lin}}^{|\ell,k|-|\ell',k'|} \mathsf{H}_{\ell'}^{k'} \quad \text{for all } (\ell',k'), (\ell,k) \in \mathcal{Q} \text{ with } |\ell',k'| \leq |\ell,k|, \quad (56)$$

where $C_{\text{lin}}, q_{\text{lin}}$ depend only on $K, L, \lambda, \theta, C_{\text{alg}}$, and the constants in (A1)–(A4), (QM).

6. QUASI-OPTIMAL COMPLEXITY

First, we briefly comment on the computational cost of a practical implementation of Algorithm A, where the polynomial degree $p \in \mathbb{N}$ of the finite element spaces (6) is arbitrary, yet fixed. On solve levels, optimal multigrid methods perform one solve step on \mathcal{T}_ℓ in $\mathcal{O}(\#\mathcal{T}_\ell)$ operations, provided the grading of the mesh hierarchy is exploited appropriately [WZ17; IMPS24]. For intermediate levels, standard smoothers have linear complexity $\mathcal{O}(\#\mathcal{T}_\ell)$, as does the computation of the refinement indicators. Dörfler marking with quasi-minimal cardinality admits an $\mathcal{O}(\#\mathcal{T}_\ell)$ implementation; see [Ste07] for $C_{\text{mark}} = 2$ and [PP20] for $C_{\text{mark}} = 1$. The cardinality-control step has at most linear cost. Finally, mesh refinement by NVB is well known to have linear complexity $\mathcal{O}(\#\mathcal{T}_\ell)$; see, e.g., [Ste08; DGS25].

Since each adaptive step depends on the entire refinement history, the computational cost up to step $(\ell, k) \in \mathcal{Q}$ is therefore, up to a multiplicative constant, given by

$$\text{cost}(\ell, k) := \sum_{\substack{(\ell',k') \in \mathcal{Q} \\ |\ell',k'| \leq |\ell,k|}} \#\mathcal{T}_{\ell'}. \quad (57)$$

A key implication of full R-linear convergence (18) is the following result, which goes back to [GHP21; BFM⁺25]. It states that convergence rates of H_ℓ^k with respect to the number of degrees of freedom $\dim \mathcal{X}_\ell \simeq \#\mathcal{T}_\ell$ and with respect to $\text{cost}(\ell, k)$ coincide.

Corollary 13 (rates = complexity). *Full R-linear convergence (18) implies*

$$\sup_{(\ell,k) \in \mathcal{Q}} (\#\mathcal{T}_\ell)^s H_\ell^k \leq \sup_{(\ell,k) \in \mathcal{Q}} \text{cost}(\ell, k)^s H_\ell^k \leq C_{\text{cost}} \sup_{(\ell,k) \in \mathcal{Q}} (\#\mathcal{T}_\ell)^s H_\ell^k \quad \text{for all } s > 0,$$

with the constant $C_{\text{cost}} := C_{\text{lin}}(1 - q_{\text{lin}}^{1/s})^{-s}$.

While Theorem 6 guarantees unconditional full R-linear convergence of Algorithm A for $C_{\text{alg}} \leq 1$, sufficiently small adaptivity parameters λ, θ additionally ensure quasi-optimal complexity, i.e., optimal convergence rates with respect to the computational cost (resp. the overall computational time). This remains true even for general C_{alg} . To formalize this, we employ approximation classes [BDD04; Ste07; CKNS08; CFPP14]. For $N \in \mathbb{N}_0$, let $\mathbb{T}(N)$ denote the set of refinements $\mathcal{T} \in \mathbb{T}$ with $\#\mathcal{T} - \#\mathcal{T}_0 \leq N$. For $s > 0$, define

$$\|u^*\|_{\mathbb{A}_s} := \sup_{N \in \mathbb{N}_0} [(N+1)^s \min_{\mathcal{T}_{\text{opt}} \in \mathbb{T}(N)} \eta_{\text{opt}}(u_{\text{opt}}^*)] \in [0, +\infty]. \quad (58)$$

One has $\|u^*\|_{\mathbb{A}_s} < +\infty$ if and only if the estimator for the exact discrete solutions converges at least with algebraic rate $s > 0$ along optimal meshes.

Theorem 14 (quasi-optimal complexity). *Assume that the solver Φ_ℓ is uniformly contractive (UC) and that the smoother Ψ_ℓ is uniformly stable (US). Let $K, L \in \mathbb{N}$, $C_{\text{mark}}, C_{\text{card}} \geq 1$, and $u_0^0 \in \mathcal{X}_0$ be arbitrary. Recall λ_{opt} from (54). Suppose that $0 < \theta \leq 1$ and $\lambda > 0$ are sufficiently small such that*

$$0 < \lambda < \theta^{1/2} \lambda_{\text{opt}} \quad \text{and} \quad 0 < \theta' := \frac{(\theta^{1/2} + \lambda/\lambda_{\text{opt}})^2}{(1 - \lambda/\lambda_{\text{opt}})^2} < (1 + C_{\text{stab}}^2 C_{\text{drel}}^2)^{-1} =: \theta_{\text{opt}}. \quad (59)$$

Then, for all $s > 0$, Algorithm A guarantees the existence of $c_{\text{opt}}, C_{\text{opt}} > 0$ satisfying

$$c_{\text{opt}} \|u^*\|_{\mathbb{A}_s} \leq \sup_{(\ell,k) \in \mathcal{Q}} \text{cost}(\ell, k)^s H_\ell^k \leq C_{\text{opt}} \max\{\|u^*\|_{\mathbb{A}_s}, H_0^0\}. \quad (60)$$

The constant c_{opt} depends only on $\#\mathcal{T}_0, s$, properties of NVB, and possibly in addition on the minimal index $\ell_0 \in \underline{\mathcal{S}}$ satisfying either $\ell_0 = \underline{\ell} < +\infty$ or $\eta_{\ell_0}(u_{\ell_0}^k) = 0$. The constant C_{opt} depends only on $s, K, L, C_{\text{card}}, C_{\text{mark}}, \theta, \lambda, q_{\text{alg}}$, properties of NVB, and the constants in (A1)–(A4), (A3⁺), (QM); for the precise dependencies see (72).

The significance of (60) is that it establishes that $\|u^*\|_{\mathbb{A}_s} < +\infty$ holds if and only if H_ℓ^k decays with algebraic rate $s > 0$ with respect to the overall computational cost. Since $s > 0$ is arbitrary, Algorithm A therefore achieves the best rate permitted by the approximation class (defined in terms of the number of elements) also with respect to the computational cost, and hence attains quasi-optimal complexity.

Remark 15. *Theorems 6 and 12 remain valid in the degenerate case $C_{\text{card}} = +\infty$, i.e., when the cardinality-control step (IV) is omitted. In contrast, the proof of Theorem 14 crucially requires this step, as without it bounding the number of marked elements on intermediate levels appears unclear.*

Remark 16. *Using a direct solver on the solve levels $\ell \in L \cdot \mathbb{N}_0$ requires at least $\mathcal{O}(\#\mathcal{T}_\ell \log(\#\mathcal{T}_\ell))$ operations. Since such solvers are uniformly contractive (UC), Theorem 14 remains applicable and, in combination with Corollary 13, yields optimal rates with respect to the number of degrees of freedom $\dim \mathcal{X}_\ell \simeq \#\mathcal{T}_\ell$. However, the computational cost up to $(\ell, k) \in \mathcal{Q}$ is no longer proportional to $\text{cost}(\ell, k)$ from (57), so quasi-optimal complexity is no longer ensured.*

Proof of Theorem 14. The lower estimate in (60) follows as in [GHPS21, Lemma 13]. The upper estimate is proved in three steps. It suffices to assume that $\|u^*\|_{\mathbb{A}_s} < +\infty$.

Step 1 (perturbation argument on solve levels). Let $\ell' \in \mathcal{S}$. For θ' as defined in (59), [CFPP14, Lemma 4.14] ensures the existence of a subset $\mathcal{R}_{\ell'} \subseteq \mathcal{T}_{\ell'}$ and constants $C_{\text{cmp}}, \tilde{C}_{\text{cmp}} > 0$, depending only on $C_{\text{stab}}, C_{\text{drel}}, C_{\text{mon}}$, such that

$$\theta' \eta_H(u_H^*)^2 \leq \eta_H(\mathcal{R}_H, u_H^*)^2 \quad \text{and} \quad \#\mathcal{R}_{\ell'} \leq \tilde{C}_{\text{cmp}} C_{\text{cmp}}^{1/s} \|u^*\|_{\mathbb{A}_s}^{1/s} \eta_{\ell'}(u_{\ell'}^*)^{-1/s}. \quad (61)$$

Using the same perturbation argument as in Step 4 of [GHPS21, Theorem 8], estimator equivalence (55) implies $\theta \eta_{\ell'}(u_{\ell'}^k)^2 \leq \eta_{\ell'}(\mathcal{R}_{\ell'}, u_{\ell'}^k)^2$. Hence, $\mathcal{R}_{\ell'}$ satisfies the Dörfler criterion with parameter θ . By **Algorithm A (III)–(IV)**, $\mathcal{M}_{\ell'} = \tilde{\mathcal{M}}_{\ell'}$ is quasi-minimal fulfilling this criterion. Together with (61) and $C_1 := C_{\text{mark}} \tilde{C}_{\text{cmp}} C_{\text{cmp}}^{1/s}$, this yields

$$\#\mathcal{M}_{\ell'} \leq C_{\text{mark}} \#\mathcal{R}_{\ell'} \stackrel{(61)}{\leq} C_1 \|u^*\|_{\mathbb{A}_s}^{1/s} \eta_{\ell'}(u_{\ell'}^*)^{-1/s}. \quad (62)$$

With $C_2 := \lambda q_{\text{alg}} / (1 - q_{\text{alg}})$, the contraction (UC) of $\Phi_{\ell'}$ and the criterion (15) yield

$$\|u_{\ell'}^* - u_{\ell'}^k\| \stackrel{(\text{UC})}{\leq} q_{\text{alg}}(1 - q_{\text{alg}})^{-1} \|u_{\ell'}^k - u_{\ell'}^{k-1}\| \stackrel{(15)}{\leq} C_2 \eta_{\ell'}(u_{\ell'}^k). \quad (63)$$

Hence, for $C_3 := [(1 + C_{\text{stab}})C_2 + 1]$, stability (A1) implies that

$$\mathsf{H}_{\ell'}^k \stackrel{(\text{A1})}{\leq} (1 + C_{\text{stab}}) \|u_{\ell'}^* - u_{\ell'}^k\| + \eta_{\ell'}(u_{\ell'}^k) \stackrel{(63)}{\leq} C_3 \eta_{\ell'}(u_{\ell'}^k). \quad (64)$$

This and the stability estimate (44) give

$$\mathsf{H}_{\ell'+1}^0 \stackrel{(44)}{\leq} C_{\text{mon}} [C_{\text{rel}}(1 + C_{\text{mon}}) + 1] \mathsf{H}_{\ell'}^k \stackrel{(64)}{\leq} C_3 C_{\text{mon}} [C_{\text{rel}}(1 + C_{\text{mon}}) + 1] \eta_{\ell'}(u_{\ell'}^k). \quad (65)$$

For $C_4 := C_1 C_3^{-1/s} C_{\text{mon}}^{-1/s} [C_{\text{rel}}(1 + C_{\text{mon}}) + 1]^{-1/s} (1 - \lambda \lambda_{\text{opt}}^{-1})^{1/s}$, the combination of (62) and (65) with estimator equivalence (55) from **Lemma 11** proves that

$$\#\mathcal{M}_{\ell'} \leq C_4 \|u^*\|_{\mathbb{A}_s}^{1/s} (\mathsf{H}_{\ell'+1}^0)^{-1/s} \quad \text{for all } \ell' \in \mathcal{S}. \quad (66)$$

Step 2 (extension to all levels). Let $\text{mod}(\ell, L)$ denote the unique integer $0 \leq r < L$ such that $\ell - r \in L \cdot \mathbb{N}_0$. Cardinality control in **Algorithm A(IV)** ensures

$$\#\mathcal{M}_{\ell'} \leq C_{\text{card}}^{\text{mod}(\ell', L)} \#\mathcal{M}_{\ell'-\text{mod}(\ell', L)} \quad \text{for all } \ell' \in \mathcal{I}. \quad (67)$$

Let $(\ell, k) \in \mathcal{Q}$ with $\mathcal{T}_{\ell} \neq \mathcal{T}_0$. Using $\#\mathcal{T}_{\ell} > \#\mathcal{T}_0$ and a mesh-closure estimate for NVB meshes [Ste08; AFF⁺13; DGS25] with constant $C_{\text{mesh}} > 0$ gives

$$\#\mathcal{T}_{\ell} - \#\mathcal{T}_0 + 1 \leq 2 (\#\mathcal{T}_{\ell} - \#\mathcal{T}_0) \leq 2C_{\text{mesh}} \left(\sum_{\ell' \in \mathcal{S}, \ell' < \ell} \#\mathcal{M}_{\ell'} + \sum_{\ell' \in \mathcal{I}, \ell' < \ell} \#\mathcal{M}_{\ell'} \right).$$

Applying (67), the second sum in the preceding formula can be bounded via

$$\sum_{\ell' \in \mathcal{I}, \ell' < \ell} \#\mathcal{M}_{\ell'} \stackrel{(67)}{\leq} \sum_{\ell' \in \mathcal{I}, \ell' < \ell} C_{\text{card}}^{\text{mod}(\ell', L)} \#\mathcal{M}_{\ell'-\text{mod}(\ell', L)} \leq \sum_{\ell' \in \mathcal{S}, \ell' < \ell} \sum_{j=1}^{L-1} C_{\text{card}}^j \#\mathcal{M}_{\ell'}.$$

With $C_5 := 2C_{\text{mesh}}[1 + \sum_{j=1}^{L-1} C_{\text{card}}^j]$, combining the previous two estimates yields

$$\#\mathcal{T}_{\ell} - \#\mathcal{T}_0 + 1 \leq C_5 \sum_{\ell' \in L \cdot \mathbb{N}_0, \ell' < \ell} \#\mathcal{M}_{\ell'} \stackrel{(66)}{\leq} C_4 C_5 \|u^*\|_{\mathbb{A}_s}^{1/s} \sum_{\ell' \in L \cdot \mathbb{N}_0, \ell' \leq \ell} (\mathsf{H}_{\ell'}^0)^{-1/s}.$$

By full R-linear convergence (56), the geometric series gives

$$\sum_{\ell' \in L \cdot \mathbb{N}_0, \ell' \leq \ell} (\mathsf{H}_{\ell'}^0)^{-1/s} \leq \sum_{\substack{(\ell', k') \in \mathcal{Q} \\ |\ell', k'| \leq |\ell, k|}} (\mathsf{H}_{\ell'}^{k'})^{-1/s} \stackrel{(56)}{\leq} C_{\text{lin}}^{1/s} (1 - q_{\text{lin}}^{1/s})^{-1} (\mathsf{H}_{\ell}^k)^{-1/s}.$$

With $C_6 := C_4 C_5 C_{\text{lin}}^{1/s} (1 - q_{\text{lin}}^{1/s})^{-1}$, the previous two displayed formulas imply

$$\#\mathcal{T}_\ell - \#\mathcal{T}_0 + 1 \leq C_6 \|u^*\|_{\mathbb{A}_s}^{1/s} (\mathsf{H}_\ell^k)^{-1/s}.$$

Exponentiation by s and rearranging the terms thus proves that

$$(\#\mathcal{T}_\ell - \#\mathcal{T}_0 + 1)^s \mathsf{H}_\ell^k \leq C_6^s \|u^*\|_{\mathbb{A}_s} \quad \text{for all } (\ell, k) \in \mathcal{Q} \text{ with } \mathcal{T}_\ell \neq \mathcal{T}_0. \quad (68)$$

Let $(\ell, k) \in \mathcal{Q}$ with $\mathcal{T}_\ell = \mathcal{T}_0$ and $\ell > 0$. In this case, no refinement has occurred and hence, $\widetilde{\mathcal{M}}_0 = \mathcal{M}_0 = \emptyset$. The quasi-minimality condition in [Algorithm A\(III\)](#) then implies $\eta_0(u_0^k) = 0$. By the stopping criterion [\(15\)](#), it holds $u_0^k = u_0^{k-1}$. The contraction [\(UC\)](#) of the solver then implies $u_0^k = u_0^*$, and thus $\eta_0(u_0^*) = 0$. Consequently, $\mathsf{H}_0^k = \eta_0(u_0^*) = 0$ and estimate [\(68\)](#) generalizes to

$$(\#\mathcal{T}_\ell - \#\mathcal{T}_0 + 1)^s \mathsf{H}_\ell^k \leq C_6^s \|u^*\|_{\mathbb{A}_s} \quad \text{for all } (\ell, k) \in \mathcal{Q} \text{ with } \ell > 0. \quad (69)$$

Finally, since [\(UC\)](#) implies $\mathsf{H}_0^k \leq \mathsf{H}_0^0$ for all $0 \leq k \leq \underline{k}[0]$, estimate [\(69\)](#) extends to

$$(\#\mathcal{T}_\ell - \#\mathcal{T}_0 + 1)^s \mathsf{H}_\ell^k \leq C_6^s \max\{\|u^*\|_{\mathbb{A}_s}, \mathsf{H}_0^0\} \quad \text{for all } (\ell, k) \in \mathcal{Q}. \quad (70)$$

Step 3 (proof of the upper estimate in [\(60\)](#)). By [\[BHP17, Lemma 22\]](#), it holds

$$\#\mathcal{T}_\ell \leq (\#\mathcal{T}_0)(\#\mathcal{T}_\ell - \#\mathcal{T}_0 + 1) \quad \text{for all } \ell \leq \underline{\ell}. \quad (71)$$

For all $(\ell', k') \in \mathcal{Q}$, [Corollary 13](#) and the combination of [\(70\)](#)–[\(71\)](#) show that

$$\text{cost}(\ell', k')^s \mathsf{H}_{\ell'}^{k'} \leq C_{\text{cost}} \sup_{(\ell, k) \in \mathcal{Q}} (\#\mathcal{T}_\ell)^s \mathsf{H}_\ell^k \stackrel{(70), (71)}{\leq} C_{\text{cost}} (\#\mathcal{T}_0)^s C_6^s \max\{\|u^*\|_{\mathbb{A}_s}, \mathsf{H}_0^0\}.$$

This concludes the proof of the upper estimate in [\(60\)](#) with constant

$$C_{\text{opt}} \leq \frac{[1 + \sum_{j=1}^{L-1} C_{\text{card}}^j]^s [(1 + C_{\text{stab}})^{\frac{q_{\text{alg}}\lambda}{1-q_{\text{alg}}} + 1} C_{\text{mark}}^s \tilde{C}_{\text{cmp}}^s C_{\text{cmp}}^2 C_{\text{lin}}^2 (\#\mathcal{T}_0)^s]}{2^{-s} C_{\text{mesh}}^{-s} C_{\text{mon}} [C_{\text{rel}}(1 + C_{\text{mon}}) + 1] (1 - \lambda \lambda_{\text{opt}}^{-1}) (1 - q_{\text{lin}}^{1/s})^{2s}}. \quad (72) \quad \square$$

7. NUMERICAL EXPERIMENTS

In the following subsections, we investigate three numerical benchmark problems in 2D (one of which is a non-symmetric convection-diffusion problem) and one Poisson problem in 3D. In view of the extensive numerical experiments in [\[MGH21\]](#), we focus on complementing aspects such as optimal convergence rates and the performance comparison with standard AFEM with inexact solvers.

7.1. Implementation. The two-dimensional experiments were conducted using the object-oriented MATLAB software package MooAFEM from [\[IP23\]](#), with the hp -robust geometric multigrid method from [\[IMPS24\]](#) employed on the solve levels of [Algorithm A](#). For the experiments in 3D, we extended the octAFEM3D software package [\[Bri21\]](#) which uses the mesh-refinement procedure from [\[Tra97\]](#).

Inhomogeneous Dirichlet boundary data $g: \partial\Omega \rightarrow \mathbb{R}$ is approximated using nodal interpolation for $d = 2$ and the Scott–Zhang quasi-interpolation [\[SZ90; AFK⁺13\]](#) for $d = 3$. This introduces an additional data oscillation term and leads to the extended estimator

$$\begin{aligned} \eta_H(T, v_H)^2 &:= |T|^{2/d} \| -\operatorname{div}(\mathbf{A} \nabla v_H - \mathbf{f}) + \mathbf{b} \cdot \nabla v_H + c v_H - f \|_{L^2(T)}^2 \\ &\quad + |T|^{1/d} \| [(\mathbf{A} \nabla v_H - \mathbf{f}) \cdot \mathbf{n}] \|_{L^2(\partial T \cap \Omega)}^2 + |T|^{1/d} \sum_{E \subseteq \partial T \cap \partial \Omega} \| (1 - \Pi_E^{p-1}) \nabla_\gamma g \|_{L^2(E)}^2. \end{aligned}$$

Therein, ∇_γ denotes the arc-length derivative for $d = 2$ and the surface gradient for $d = 3$, and Π_E^{p-1} is the $L^2(E)$ -orthogonal projection onto the space of polynomials of degree $p - 1$ on the boundary edge $E \subseteq \partial\Omega$. For further details, we refer to [\[AFK⁺13; FPP14; BC17\]](#).

All experiments employ [Algorithm A](#) with marking parameter $C_{\text{mark}} = 1$, cardinality control constant $C_{\text{card}} = 10$, initial guess $u_0^0 = 0$, and, unless stated otherwise, polynomial degree

$p = 2$ and bulk parameter $\theta = 0.5$. The stopping parameter $0 < \lambda$ reflects the balance between discretization and algebra error. The reader is referred to [GHP21; BFM⁺25; BMP24] for a numerical investigation and discussion on the choice of λ . We compare the *Richardson* iteration (RI), *Gauss–Seidel* iteration (GS), and *PCG with incomplete Cholesky preconditioning* (PCG-iChol) for the intermediate-level smoothing. Moreover, we employ the *identity* operator (ID) on intermediate mesh levels, corresponding to omitting the smoothing iteration. All these choices are uniformly stable (US) with $C_{\text{alg}} = 1$; cf. [subsection 3.2](#). For the non-symmetric problem, we employ the uniformly stable Zarantonello symmetrization according to [Proposition 3](#).

As a reference for the runtime improvements, we employ the standard AFEM [GHP21; BFM⁺25] with inexact algebraic solver realized by the S-AFEM [Algorithm A](#) with $L = 1$. We measure the algebraic computation time required to reach a given accuracy in terms of the energy error $\|u^* - u_\ell^k\|$. Let $\text{solutionTime}(\ell)$ denote the time required by [Algorithm A](#) on level ℓ to execute step (I) if $\ell \in L \cdot \mathbb{N}_0$ or step (II) if $\ell \notin L \cdot \mathbb{N}_0$. The remaining steps (III)–(IV) are excluded from the measurement as they are identical for AFEM and S-AFEM and, in practice, the algebraic solution dominates the overall runtime. The cumulative solution time up to level ℓ reads $\text{cumulativeSolutionTime}(\ell) := \sum_{\ell'=0}^{\ell} \text{solutionTime}(\ell')$. We determine a function $e \mapsto \text{cumulativeSolutionTime}_{\text{ref}}(e)$ by piecewise affine interpolation in log-log scale of points (e_ℓ, t_ℓ) with the energy error $e_\ell := \|u^* - u_\ell^k\|$ and $t_\ell := \text{solutionTime}(\ell)$ on the level ℓ of the AFEM reference computation ($L = 1$). Evaluating this function at the energy error $\|u^* - u_\ell^k\|$ attained by S-AFEM allows to define the *algebraic speed-up factor* of S-AFEM in relation to AFEM by

$$S_\ell := \frac{\text{cumulativeSolutionTime}_{\text{ref}}(\|u^* - u_\ell^k\|)}{\text{cumulativeSolutionTime}(\ell)} \quad \text{for } \ell \in \mathbb{N}_0, \quad (73)$$

For all timing measurements, three independent runs were performed and the reported times correspond to the run attaining the median total runtime.

7.2. 2D Poisson problem with interface load. We consider the Z-shaped domain $\Omega = (-1, 1)^2 \setminus \text{conv}\{(0, 0), (-1, 0), (-1, -1)\}$ and seek $u^* \in H_0^1(\Omega)$ satisfying

$$-\Delta u^* = \text{div}(\chi_\omega(1, 1)^\top) \text{ in } \Omega, \quad (74)$$

where $\chi_\omega: \Omega \rightarrow \{0, 1\}$ denotes the indicator function of $\omega := \text{conv}\{(1, 0), (1, 1), (0, 1)\}$. A moderate choice of $\lambda = 0.1$ is sufficient for the diffusion problem at hand.

[Figure 3](#) (center) shows that [Algorithm A](#) with Gauss–Seidel smoothing resolves both types of singularities, the one at the re-entrant corner singularity and the one induced by the right-hand side in (74). The resulting mesh is essentially comparable to that obtained for the standard AFEM ($L = 1$), see [Figure 3](#) (right). In contrast, the identity operator in S-AFEM yields noticeably inferior meshes; see [Figure 3](#) (left). The choices of Gauss–Seidel smoothing or the identity operator in [Algorithm A](#) result in optimal convergence rates with respect to the number of degrees of freedom and the cumulative runtime as shown in [Figure 4](#). This confirms the theoretical result of [Theorem 14](#). Moreover, [Table 1](#) compares estimator-weighted cumulative runtimes

$$\eta_\ell(u_\ell^k) \text{cumulativeTime}(\ell)^{p/2}, \quad (75)$$

where $\text{cumulativeTime}(\ell)$ denotes the cumulative runtime of [Algorithm A](#) up to level ℓ , for different smoothers, polynomial degrees p , and parameters L, K . Since estimator equivalence (55) from [Lemma 11](#) holds exclusively on solve levels, the S-AFEM algorithm is stopped for $\ell \in L \cdot \mathbb{N}_0$ as soon as the prescribed tolerance $\eta_\ell(u_\ell^k) < 2 \cdot 10^{-4}$ is reached. We observe that intermediate-level smoothing consistently yields significant runtime reductions, emphasizing the computational efficiency of S-AFEM compared to standard AFEM ($L = 1$).

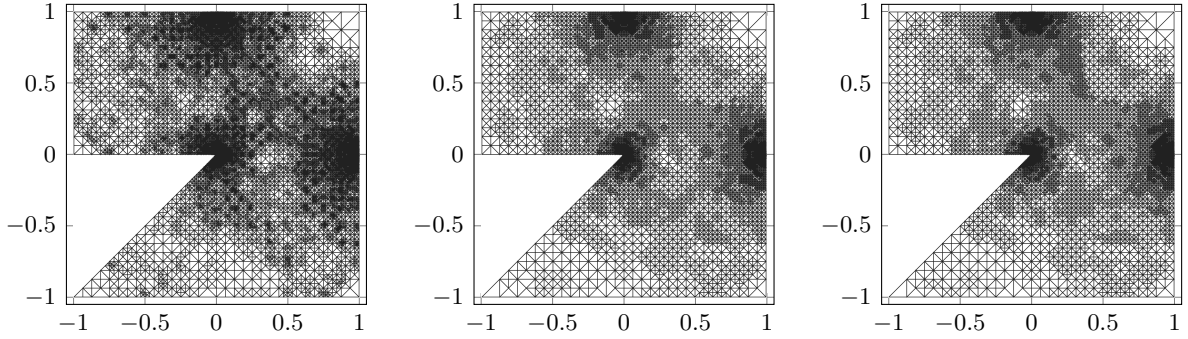


FIGURE 3. Final meshes \mathcal{T}_{15} on level $\ell = 15$ generated by [Algorithm A](#) for the Poisson problem (74) with $L = 5$ and ID (left), $L = 5 = K$ and GS (center), and $L = 1$ (AFEM, right).

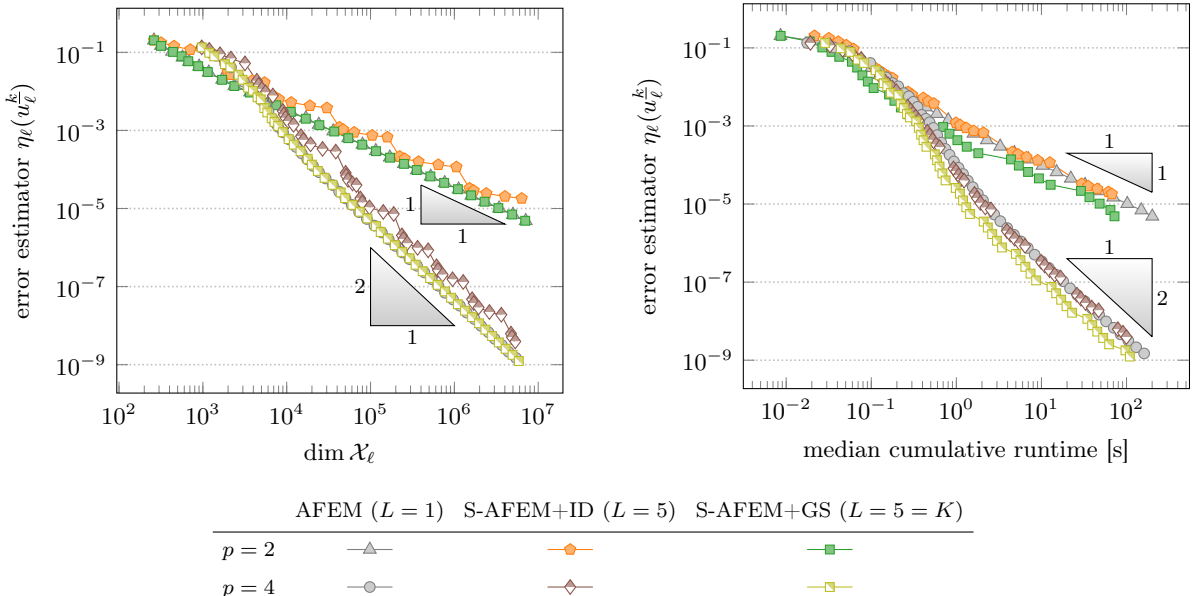


FIGURE 4. Convergence history of the error estimator $\eta_\ell(u_\ell^k)$ for various polynomial degrees p in [Algorithm A](#) applied to the Poisson problem (74).

TABLE 1. Estimator-weighted cumulative runtime from (75) (values in 10^{-5}) for the Poisson problem (74) with various smoothers and parameters p, L, K . The fastest runtime in each row is highlighted in blue.

S-AFEM		Richardson		Gauss-Seidel		PCG-iChol		AFEM
		$L = 5$	$L = 10$	$L = 5$	$L = 10$	$L = 5$	$L = 10$	
$p = 2$	$K = 5$	64.76	78.32	60.97	61.30	56.40	53.05	98.66
$p = 2$	$K = 10$	62.70	71.90	59.40	59.71	57.57	54.42	98.66
$p = 3$	$K = 5$	7.31	19.01	6.87	6.73	6.02	5.45	14.73
$p = 3$	$K = 10$	7.42	10.62	5.94	5.60	6.29	5.77	14.73
$p = 4$	$K = 5$	4.93	11.41	5.85	3.65	6.83	3.91	12.60
$p = 4$	$K = 10$	3.74	7.38	3.84	4.17	6.12	5.43	12.60

TABLE 2. Algebraic speed-up factors S_ℓ defined in (73) in the Kellogg problem (76). The factors are evaluated on the final mesh with respect to the overall stopping criterion $\dim \mathcal{X}_\ell \geq 9 \cdot 10^5$. The largest value of S_ℓ in each row is highlighted in blue. Within each p -block, the largest value of S_ℓ is highlighted in yellow, and in green when both coincide.

	$p = 1$		$p = 2$		$p = 3$		$p = 4$	
	$L = 5$	$L = 10$						
GS ($K = 10$)	0.19	0.07	1.02	0.68	1.48	1.11	1.43	0.85
GS ($K = 20$)	0.19	0.09	1.04	0.80	1.42	1.22	1.40	1.07
GS ($K = 30$)	0.19	0.10	1.01	0.93	1.41	1.17	1.35	1.10
PCG-iChol ($K = 10$)	0.26	0.12	1.85	2.49	2.04	2.16	1.90	1.61
PCG-iChol ($K = 20$)	0.73	0.68	11.48	14.41	11.39	12.97	8.65	9.58
PCG-iChol ($K = 30$)	1.77	1.77	15.28	19.03	11.58	13.24	8.07	8.88

7.3. 2D Kellogg problem. We consider the classical Kellogg problem on the square domain $\Omega = (-1, 1)^2$ seeking $u^* \in H^1(\Omega)$ satisfying

$$-\operatorname{div}(\alpha \nabla u^*) = 0 \text{ in } \Omega \quad \text{subject to} \quad u^* = g \text{ on } \partial\Omega, \quad (76)$$

where the diffusion coefficient $\alpha : \Omega \rightarrow \mathbb{R}$ is given by $\alpha(x_1, x_2) = 161.4476387975881$ if $x_1 x_2 > 0$ and $\alpha(x_1, x_2) = 1$ otherwise. The known exact solution from [Kel74] satisfies $u^* \in H^{1,1-\varepsilon}(\Omega)$ for all $\varepsilon > 0$ and prescribes the Dirichlet boundary data $g : \partial\Omega \rightarrow \mathbb{R}$; see, e.g., [BMP24, Section 3] for the explicit expression. The challenging singularity at the origin motivates a smaller stopping parameter $\lambda = 0.005$ to ensure a sufficiently accurate approximation on the solve levels.

Table 2 reports the resulting algebraic speed-up factors measured on the final mesh. Intermediate-level smoothing with PCG-iChol yields consistently large speed-ups, which become increasingly stronger for $2 \leq p$, reaching values of up to $S_\ell \approx 19$ for $p = 2$. For $p = 1$, the effect is markedly weaker and often negligible, with speed-up factors close to or even below one, indicating that the performance difference between PCG-iChol smoothing and the multigrid solver is less pronounced. Intermediate-level Gauss–Seidel smoothing produces only moderate improvements for the strongly singular Kellogg problem and increasing the number of intermediate smoothing steps K does not lead to further gains. Undisplayed numerical experiments suggest that this inferior performance stems from a high number of solver iterations on the solve levels needed to compensate the poor algebraic approximation on the intermediate levels.

7.4. 2D convection-diffusion on L-shaped domain. On the L-shaped domain $\Omega = (-1, 1)^2 \setminus ([0, 1] \times [-1, 0])$, we consider

$$-\Delta u^* + (5, 5)^\top \cdot \nabla u^* = 1 \text{ in } \Omega \quad \text{subject to} \quad u^* = 0 \text{ on } \partial\Omega. \quad (77)$$

Throughout this subsection, we choose $\lambda = 0.05$, $\theta = 0.5$ and the Zarantonello damping parameter $\delta = 0.5$. We construct uniformly stable iterative methods via Zarantonello symmetrization according to Proposition 3. For $v_H \in \mathcal{X}_H$, let $\Theta_H^{\text{MG}}(v_H)$ and $\Theta_H^{\text{PCG}}(v_H)$ denote the iteration operators of the multigrid method from [IMPS24] and of PCG-iChol, respectively, applied to the symmetrized problem (11). For the non-symmetric system (7), define the iteration operators

$$\Phi_H(v_H) := (\Theta_H^{\text{MG}}(v_H))^2(v_H) \quad \text{and} \quad \Psi_H(v_H) := (\Theta_H^{\text{PCG}}(v_H))^4(v_H), \quad (78)$$

i.e., applying, e.g., Φ_H corresponds to two multigrid iterations on the symmetrized problem (11). The adaptive meshes computed by S-AFEM are displayed in Figure 5 and exhibit slight under-refinement at the boundary layer for $L > 1$ which, however, does not impact on the optimal convergence rates with respect to the cumulative runtime in Figure 6 (left). The number of solver iterations on the solve levels remains moderate; see Figure 6 (right). Finally, Table 3 indicates that, for the non-symmetric problem (77), S-AFEM yields noticeable computational

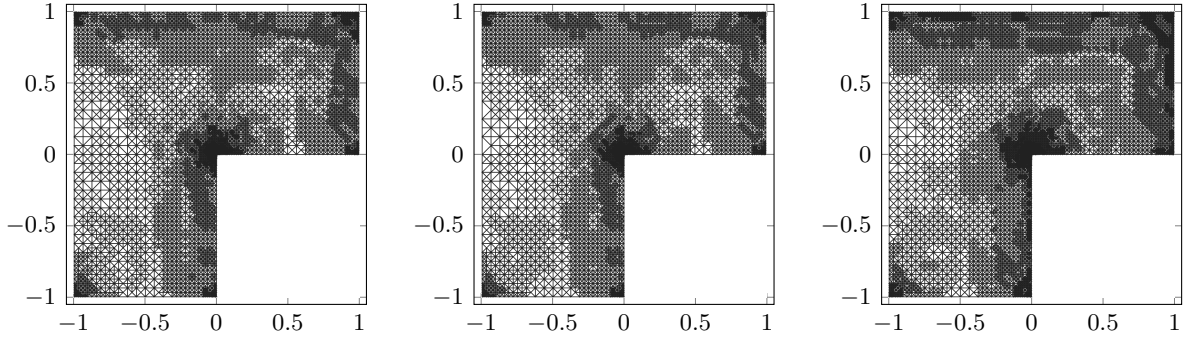


FIGURE 5. Final meshes \mathcal{T}_{20} on level $\ell = 20$ generated by [Algorithm A](#) for the convection-diffusion problem (77) with $p = 3$ for $K = 3, L = 5$ (left), $K = 3, L = 10$ (center), and $L = 1$ (AFEM, right).

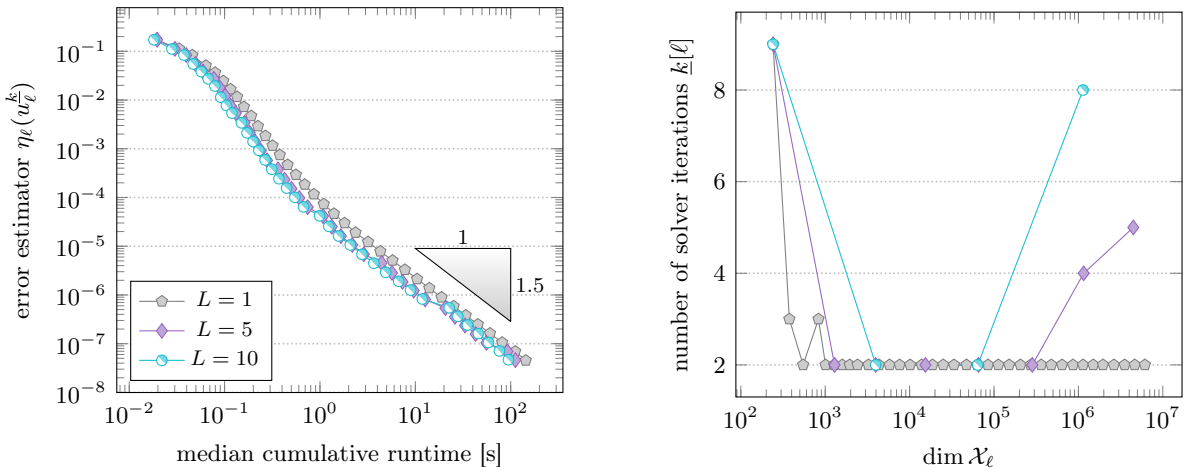


FIGURE 6. Convergence of the error estimator $\eta_\ell(u_\ell^k)$ (left) and the number of solver iterations (right) on solve levels for the convection-diffusion problem (77) with $p = 3$ for $K = 3$.

TABLE 3. Estimator-weighted cumulative runtime from (75) (values in 10^{-5}) of [Algorithm A](#) for the convection-diffusion problem (77). The fastest runtime in each row is highlighted in blue.

S-AFEM	$L = 5$			$L = 10$			$L = 1$
	$K = 1$	$K = 3$	$K = 5$	$K = 1$	$K = 3$	$K = 5$	
$p = 2$	96.14	104.58	79.67	100.44	80.93	92.45	132.60
$p = 3$	6.16	7.67	5.85	5.61	6.21	6.05	13.97
$p = 4$	2.54	2.44	2.46	2.13	2.90	2.87	8.39

advantages over standard AFEM ($L = 1$), although less significant than for the previous symmetric problems.

7.5. 3D Poisson problem on Fichera cube. In three spatial dimensions, we consider the Poisson problem on the Fichera cube $\Omega = (-1, 1)^3 \setminus [0, 1]^3$ given by

$$-\Delta u^* = f \text{ in } \Omega \quad \text{subject to} \quad u^* = g \text{ on } \partial\Omega, \quad (79)$$

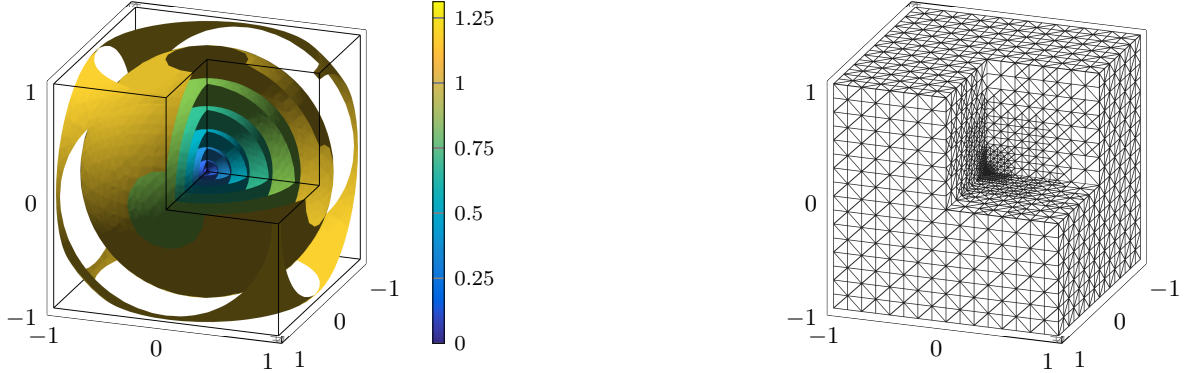


FIGURE 7. Isosurfaces of the S-AFEM approximation u_{30}^* (left) and final mesh with 97188 simplices (right) on level $\ell = 30$ generated by [Algorithm A](#) with $K = 5$ Gauss–Seidel smoothing iterations and $L = 10$ for the 3D Fichera problem (79).

where the forcing term $f: \Omega \rightarrow \mathbb{R}$ and the Dirichlet data $g: \partial\Omega \rightarrow \mathbb{R}$ are chosen as in [MGH21] so that the exact solution in spherical coordinates is $u^*(r, \varphi, \theta) = r^{1/2}$. We fix $\theta = 0.3, p = 1$ and use MATLAB’s built-in direct solver `mldivide` on the solve levels.

Figure 7 illustrates the S-AFEM approximation and the adapted final mesh, showing that few non-preconditioned intermediate smoothing steps yield effective adaptivity near the origin. We investigate the algebraic speed-up factors S_ℓ from (73) in Figure 8 and observe that S-AFEM also yields substantial speed-ups for the 3D problem, achieving runtime improvements of up to $S_\ell \approx 8$ relative to standard AFEM.

Finally, we propose a practice-oriented strategy for the use of S-AFEM in realistic computations. Given a target tolerance $0 < \tau$ for the error estimator, perform a moderate number of initial solve-estimate-mark-refine loops with very inexpensive direct solves on coarse meshes. Based on the resulting log-log relation between the estimator and the number of degrees of freedom, a linear regression is used to predict the number of degrees of freedom required to reach τ . The adaptive loop is then continued using only a fixed number of smoothing steps per mesh, as in [Algorithm A](#) on intermediate mesh levels, until this threshold is reached. We terminate with a final exact (or sufficiently accurate) solve. This allows to acceptably predict the number of intermediate smoothing levels in the S-AFEM algorithm as used in [MGH21]. Figure 9 illustrates the efficiency of the strategy for the model problem at hand.

7.6. Conclusion. Adaptive mesh-refinement algorithms with inexact algebraic solvers allow to efficiently compute finite element solutions to PDEs in quasi-optimal runtime. The numerical experiments revealed that intermediate smoothing steps suffice to generate comparably good meshes and further reduce the overall computational effort considerably. Even very inexpensive standard algebraic iterations without or with light preconditioning yield sound results. This is particularly important in practical computations, where one is interested in a good approximation only on a final mesh rather than on all intermediate meshes. We demonstrated that a few number of accurate solution steps in the beginning can be used to predict the required number of smoothing steps to compute this final mesh.

REFERENCES

- [AFF⁺13] M. Aurada, M. Feischl, T. Führer, M. Karkulik, and D. Praetorius. Efficiency and optimality of some weighted-residual error estimator for adaptive 2D boundary element methods. *Comput. Methods Appl. Math.*, 13(3):305–332, 2013. doi: [10.1515/cmam-2013-0010](https://doi.org/10.1515/cmam-2013-0010).
- [AFK⁺13] M. Aurada, M. Feischl, J. Kemetmüller, M. Page, and D. Praetorius. Each $H^{1/2}$ -stable projection yields convergence and quasi-optimality of adaptive FEM with inhomogeneous Dirichlet data in \mathbb{R}^d . *ESAIM Math. Model. Numer. Anal.*, 47(4):1207–1235, 2013. doi: [10.1051/m2an/2013069](https://doi.org/10.1051/m2an/2013069).

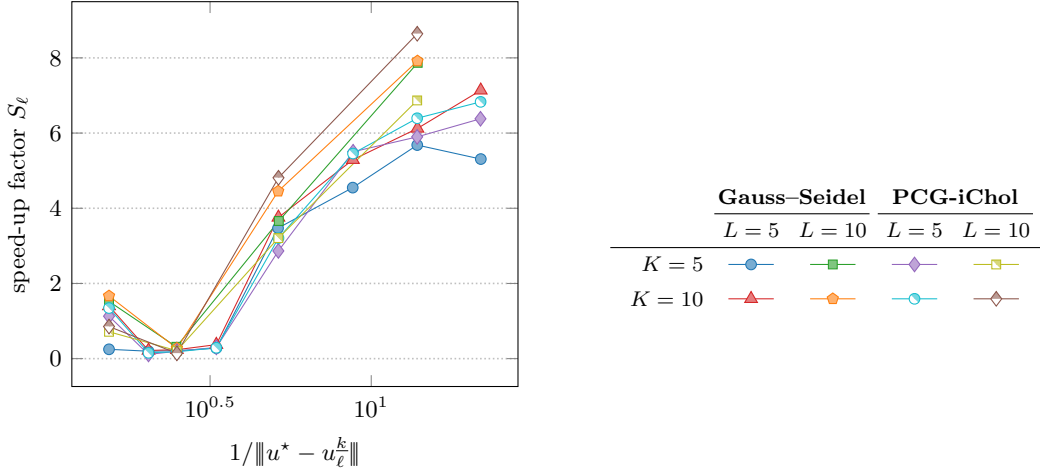
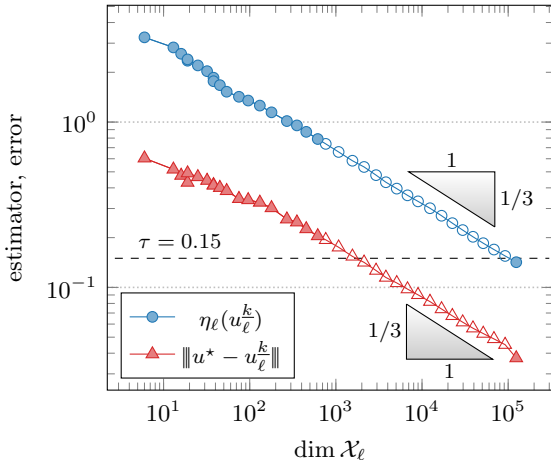


FIGURE 8. Algebraic speed-up factors S_ℓ from (73) for $\ell \in L \cdot \mathbb{N}_0$ of Algorithm A relative to standard AFEM ($L = 1$) for the 3D Fichera problem (79).



	AFEM	S-AFEM
Initial 20 solves	0.045s	0.052s
Intermediate solves	14.49s	0.169s
Final solve	5.82s	6.84s
Intermediate speed-up		85.5
Total speed-up		2.9

FIGURE 9. Convergence history (left) and solution time (right) for the 3D Fichera problem (79). After direct solves on the first 20 meshes, reaching estimator threshold $\tau = 0.15$ is predicted to require $\dim \mathcal{X}_\ell = 109215$. Thereafter, S-AFEM applies $K = 5$ Gauss–Seidel iterations per mesh until a final direct solve is performed. The AFEM reference is computed with $L = 1$ up to the predicted threshold. Hollow markers indicate smoothing.

- [AO00] M. Ainsworth and J. T. Oden. *A posteriori error estimation in finite element analysis*. John Wiley & Sons, 2000. doi: [10.1002/9781118032824](https://doi.org/10.1002/9781118032824).
- [BC17] P. Bringmann and C. Carstensen. h -adaptive least-squares finite element methods for the 2D Stokes equations of any order with optimal convergence rates. *Comput. Math. Appl.*, 74(8):1923–1939, 2017. doi: [10.1016/j.camwa.2017.02.019](https://doi.org/10.1016/j.camwa.2017.02.019).
- [BDD04] P. Binev, W. Dahmen, and R. DeVore. Adaptive finite element methods with convergence rates. *Numer. Math.*, 97(2):219–268, 2004. doi: [10.1007/s00211-003-0492-7](https://doi.org/10.1007/s00211-003-0492-7).
- [BDK12] L. Bejenki, L. Diening, and C. Kreuzer. Optimality of an adaptive finite element method for the p -Laplacian equation. *IMA J. Numer. Anal.*, 32(2):484–510, 2012. doi: [10.1093/imanum/drr016](https://doi.org/10.1093/imanum/drr016).
- [BFM⁺25] P. Bringmann, M. Feischl, A. Miraçi, D. Praetorius, and J. Streitberger. On full linear convergence and optimal complexity of adaptive FEM with inexact solver. *Comput. Math. Appl.*, 180:102–129, 2025. doi: [10.1016/j.camwa.2024.12.013](https://doi.org/10.1016/j.camwa.2024.12.013).
- [BHP17] A. Bespalov, A. Haberl, and D. Praetorius. Adaptive FEM with coarse initial mesh guarantees optimal convergence rates for compactly perturbed elliptic problems. *Comput. Methods Appl. Mech. Engrg.*, 317:318–340, 2017. doi: [10.1016/j.cma.2016.12.014](https://doi.org/10.1016/j.cma.2016.12.014).

[BIM⁺24] M. Brunner, M. Innerberger, A. Miraçi, D. Praetorius, J. Streitberger, and P. Heid. Corrigendum to: Adaptive FEM with quasi-optimal overall cost for nonsymmetric linear elliptic PDEs. *IMA Journal of Numerical Analysis*, 44(3):1903–1909, 2024. doi: [10.1093/imanum/drad103](https://doi.org/10.1093/imanum/drad103).

[BJR95] R. Becker, C. Johnson, and R. Rannacher. Adaptive error control for multigrid finite element methods. *Computing*, 55(4):271–288, 1995. doi: [10.1007/BF02238483](https://doi.org/10.1007/BF02238483).

[BMP24] P. Bringmann, A. Miraçi, and D. Praetorius. Chapter Four - Iterative solvers in adaptive FEM: Adaptivity yields quasi-optimal computational runtime. In *Error Control, Adaptive Discretizations, and Applications, Part 2*. Volume 59, Advances in Applied Mechanics, pages 147–212. Elsevier, 2024. doi: [10.1016/bs.aams.2024.08.002](https://doi.org/10.1016/bs.aams.2024.08.002).

[Bri21] P. Bringmann. octAFEM3D Software package for PhD thesis “Adaptive least-squares finite element method with optimal convergence rates”, 2021. doi: [10.18452/22346](https://doi.org/10.18452/22346).

[CDD01] A. Cohen, W. Dahmen, and R. DeVore. Adaptive wavelet methods for elliptic operator equations: convergence rates. *Math. Comp.*, 70(233):27–75, 2001. doi: [10.1090/S0025-5718-00-01252-7](https://doi.org/10.1090/S0025-5718-00-01252-7).

[CDD03] A. Cohen, W. Dahmen, and R. DeVore. Adaptive wavelet schemes for nonlinear variational problems. *SIAM J. Numer. Anal.*, 41(5):1785–1823, 2003. doi: [10.1137/s0036142902412269](https://doi.org/10.1137/s0036142902412269).

[CFPP14] C. Carstensen, M. Feischl, M. Page, and D. Praetorius. Axioms of adaptivity. *Comput. Math. Appl.*, 67(6):1195–1253, 2014. doi: [10.1016/j.camwa.2013.12.003](https://doi.org/10.1016/j.camwa.2013.12.003).

[CG12] C. Carstensen and J. Gedicke. An adaptive finite element eigenvalue solver of asymptotic quasi-optimal computational complexity. *SIAM J. Numer. Anal.*, 50(3):1029–1057, 2012. doi: [10.1137/090769430](https://doi.org/10.1137/090769430).

[CKNS08] J. M. Cascón, C. Kreuzer, R. H. Nochetto, and K. G. Siebert. Quasi-optimal convergence rate for an adaptive finite element method. *SIAM J. Numer. Anal.*, 46(5):2524–2550, 2008. doi: [10.1137/07069047X](https://doi.org/10.1137/07069047X).

[CN12] J. M. Cascón and R. H. Nochetto. Quasioptimal cardinality of AFEM driven by nonresidual estimators. *IMA J. Numer. Anal.*, 32(1):1–29, 2012. doi: [10.1093/imanum/drr014](https://doi.org/10.1093/imanum/drr014).

[CS07] A. Chaillou and M. Suri. A posteriori estimation of the linearization error for strongly monotone nonlinear operators. *J. Comput. Appl. Math.*, 205(1):72–87, 2007. doi: [10.1016/j.cam.2006.04.041](https://doi.org/10.1016/j.cam.2006.04.041).

[DGS25] L. Diening, L. Gehringer, and J. Storn. Adaptive mesh refinement for arbitrary initial triangulations. *Found. Comput. Math.*, 2025. doi: [10.1007/s10208-025-09698-7](https://doi.org/10.1007/s10208-025-09698-7).

[DK08] L. Diening and C. Kreuzer. Linear convergence of an adaptive finite element method for the p -Laplacian equation. *SIAM J. Numer. Anal.*, 46(2):614–638, 2008. doi: [10.1137/070681508](https://doi.org/10.1137/070681508).

[Dör96] W. Dörfler. A convergent adaptive algorithm for Poisson’s equation. *SIAM J. Numer. Anal.*, 33(3):1106–1124, 1996. doi: [10.1137/0733054](https://doi.org/10.1137/0733054).

[Fei22] M. Feischl. Inf-sup stability implies quasi-orthogonality. *Math. Comp.*, 91(337):2059–2094, 2022. doi: [10.1090/mcom/3748](https://doi.org/10.1090/mcom/3748).

[FFP14] M. Feischl, T. Führer, and D. Praetorius. Adaptive FEM with optimal convergence rates for a certain class of nonsymmetric and possibly nonlinear problems. *SIAM J. Numer. Anal.*, 52(2):601–625, 2014. doi: [10.1137/120897225](https://doi.org/10.1137/120897225).

[FPP14] M. Feischl, M. Page, and D. Praetorius. Convergence and quasi-optimality of adaptive FEM with inhomogeneous Dirichlet data. *J. Comput. Appl. Math.*, 255:481–501, 2014. doi: [10.1016/j.cam.2013.06.009](https://doi.org/10.1016/j.cam.2013.06.009).

[GHP18] G. Gantner, A. Haberl, D. Praetorius, and B. Stiftner. Rate optimal adaptive FEM with inexact solver for nonlinear operators. *IMA J. Numer. Anal.*, 38(4):1797–1831, 2018. doi: [10.1093/imanum/drx050](https://doi.org/10.1093/imanum/drx050).

[GHP21] G. Gantner, A. Haberl, D. Praetorius, and S. Schimanko. Rate optimality of adaptive finite element methods with respect to overall computational costs. *Math. Comp.*, 90(331):2011–2040, 2021. doi: [10.1090/mcom/3654](https://doi.org/10.1090/mcom/3654).

[GMZ12] E. Garau, P. Morin, and C. Zuppa. Quasi-Optimal Convergence Rate of an AFEM for quasi-linear Problems of Monotone Type. *Numer. Math: Theory, Meth. Appl.*, 5(2):131–156, 2012. doi: [10.4208/nmtma.2012.m1023](https://doi.org/10.4208/nmtma.2012.m1023).

[GV13] G. H. Golub and C. F. Van Loan. *Matrix computations*. Johns Hopkins University Press, 4th edition, 2013. doi: [10.56021/9781421407944](https://doi.org/10.56021/9781421407944).

[Hac16] W. Hackbusch. *Iterative solution of large sparse systems of equations*. Springer Cham, 2nd edition, 2016. doi: [10.1007/978-3-319-28483-5](https://doi.org/10.1007/978-3-319-28483-5).

[IMPS24] M. Innerberger, A. Miraçi, D. Praetorius, and J. Streitberger. hp -robust multigrid solver on locally refined meshes for FEM discretizations of symmetric elliptic PDEs. *ESAIM Math. Model. Numer. Anal.*, 58(1):247–272, 2024. doi: [10.1051/m2an/2023104](https://doi.org/10.1051/m2an/2023104).

[IP23] M. Innerberger and D. Praetorius. MooAFEM: an object oriented Matlab code for higher-order adaptive FEM for (nonlinear) elliptic PDEs. *Appl. Math. Comput.*, 442:127731, 2023. doi: [10.1016/j.amc.2022.127731](https://doi.org/10.1016/j.amc.2022.127731).

[Kel74] R. B. Kellogg. On the Poisson equation with intersecting interfaces. *Applicable Anal.*, 4:101–129, 1974. doi: [10.1080/00036817408839086](https://doi.org/10.1080/00036817408839086).

[KPP13] M. Karkulik, D. Pavlicek, and D. Praetorius. On 2D newest vertex bisection: optimality of mesh-closure and H^1 -stability of L_2 -projection. *Constr. Approx.*, 38(2):213–234, 2013. doi: [10.1007/s00365-013-9192-4](https://doi.org/10.1007/s00365-013-9192-4).

[LS25] Y. Li and H. Shui. Smoother-type a posteriori error estimates for finite element methods, 2025. arXiv: [2510.07677 \[math.NA\]](https://arxiv.org/abs/2510.07677).

[LZ21] Y. Li and L. Zikatanov. A posteriori error estimates of finite element methods by preconditioning. *Comput. Math. Appl.*, 91:192–201, 2021. doi: [10.1016/j.camwa.2020.08.001](https://doi.org/10.1016/j.camwa.2020.08.001).

[MGH21] O. Mulita, S. Giani, and L. Heltai. Quasi-optimal mesh sequence construction through smoothed adaptive finite element methods. *SIAM J. Sci. Comput.*, 43(3):A2211–A2241, 2021. doi: [10.1137/19M1262097](https://doi.org/10.1137/19M1262097).

[MN05] K. Mekchay and R. H. Nochetto. Convergence of adaptive finite element methods for general second order linear elliptic PDEs. *SIAM J. Numer. Anal.*, 43(5):1803–1827, 2005. doi: [10.1137/04060929X](https://doi.org/10.1137/04060929X).

[MNS00] P. Morin, R. H. Nochetto, and K. G. Siebert. Data oscillation and convergence of adaptive FEM. *SIAM J. Numer. Anal.*, 38(2):466–488, 2000. doi: [10.1137/S0036142999360044](https://doi.org/10.1137/S0036142999360044).

[PP20] C.-M. Pfeiler and D. Praetorius. Dörfler marking with minimal cardinality is a linear complexity problem. *Math. Comp.*, 89(326):2735–2752, 2020. doi: [10.1090/mcom/3553](https://doi.org/10.1090/mcom/3553).

[Ste07] R. Stevenson. Optimality of a standard adaptive finite element method. *Found. Comput. Math.*, 7(2):245–269, 2007. doi: [10.1007/s10208-005-0183-0](https://doi.org/10.1007/s10208-005-0183-0).

[Ste08] R. Stevenson. The completion of locally refined simplicial partitions created by bisection. *Math. Comp.*, 77(261):227–241, 2008. doi: [10.1090/S0025-5718-07-01959-X](https://doi.org/10.1090/S0025-5718-07-01959-X).

[SZ90] L. R. Scott and S. Zhang. Finite element interpolation of nonsmooth functions satisfying boundary conditions. *Math. Comp.*, 54(190):483–493, 1990. doi: [10.2307/2008497](https://doi.org/10.2307/2008497).

[Tra97] C. T. Traxler. An algorithm for adaptive mesh refinement in n dimensions. *Computing*, 59(2):115–137, 1997. doi: [10.1007/BF02684475](https://doi.org/10.1007/BF02684475).

[Vee02] A. Veeser. Convergent adaptive finite elements for the nonlinear Laplacian. *Numer. Math.*, 92(4):743–770, 2002. doi: [10.1007/s002110100377](https://doi.org/10.1007/s002110100377).

[Ver13] R. Verfürth. *A posteriori error estimation techniques for finite element methods*. Oxford University Press, Oxford, 2013. doi: [10.1093/acprof:oso/9780199679423.001.0001](https://doi.org/10.1093/acprof:oso/9780199679423.001.0001).

[WZ17] J. Wu and H. Zheng. Uniform convergence of multigrid methods for adaptive meshes. *Appl. Numer. Math.*, 113:109–123, 2017. doi: [10.1016/j.apnum.2016.11.005](https://doi.org/10.1016/j.apnum.2016.11.005).

[Zar60] E. H. Zarantonello. Solving functional equations by contractive averaging. Technical report 160, Mathematics Research Center, University of Wisconsin, 1960.

[Zei90] E. Zeidler. *Nonlinear functional analysis and its applications: II/B: Nonlinear monotone operators*. Springer New York, 1990. doi: [10.1007/978-1-4612-0981-2](https://doi.org/10.1007/978-1-4612-0981-2).

APPENDIX A. PROOFS OF PROPOSITION 3 AND THEOREM 12

Proof of Proposition 3. We adapt the reasoning from [BIM⁺24, Section 2] to the present setting. By the triangle inequality and the definition of Ψ_H , it follows that

$$\|u_H^* - \Psi_H(v_H)\| \leq \|u_H^* - \mathcal{Z}_H^\delta v_H\| + \|\mathcal{Z}_H^\delta v_H - (\Theta_H(v_H))^J(v_H)\|. \quad (80)$$

Since $\mathcal{Z}_H^\delta u_H^* = u_H^*$, the Lipschitz continuity (12) of \mathcal{Z}_H^δ yields

$$\|u_H^* - \mathcal{Z}_H^\delta v_H\| \stackrel{(12)}{\leq} C[\delta] \|u_H^* - v_H\|. \quad (81)$$

For the second term in (80), uniform stability (13) of $\Theta_H(v_H)$ gives

$$\begin{aligned} \|\mathcal{Z}_H^\delta v_H - (\Theta_H(v_H))^J(v_H)\| &\stackrel{(13)}{\leq} C_{\text{alg}}^J \|\mathcal{Z}_H^\delta v_H - v_H\| \\ &\leq C_{\text{alg}}^J (\|u_H^* - \mathcal{Z}_H^\delta v_H\| + \|u_H^* - v_H\|) \stackrel{(81)}{\leq} C_{\text{alg}}^J (C[\delta] + 1) \|u_H^* - v_H\|. \end{aligned} \quad (82)$$

Combining (80) and (82) establishes (14). Finally, an elementary calculation shows that $0 < \delta < 2C_{\text{ell}}^2/C_{\text{bnd}}^2$ implies $0 < C[\delta] < 1$. Thus, for $J \in \mathbb{N}_0$ sufficiently large, Ψ_H is uniformly contractive (UC). This concludes the proof. \square

Proof of Theorem 12. Let $\ell \in \mathcal{S}$ and write $\ell = jL$ with $j \in \mathbb{N}_0$. Contraction (UC) of Φ_ℓ yields

$$\|u_{jL}^* - u_{jL}^{k-1}\| \leq \|u_{jL}^* - u_{jL}^k\| + \|u_{jL}^k - u_{jL}^{k-1}\| \stackrel{(UC)}{\leq} q_{\text{alg}} \|u_{jL}^* - u_{jL}^{k-1}\| + \|u_{jL}^k - u_{jL}^{k-1}\|. \quad (83)$$

A rearrangement of the previous estimate together with the stopping criterion (15) implies

$$\|u_{jL}^* - u_{jL}^k\| \stackrel{(UC)}{\leq} q_{\text{alg}} \|u_{jL}^* - u_{jL}^{k-1}\| \stackrel{(83)}{\leq} \frac{q_{\text{alg}}}{1 - q_{\text{alg}}} \|u_{jL}^k - u_{jL}^{k-1}\| \stackrel{(15)}{\leq} \lambda \frac{q_{\text{alg}}}{1 - q_{\text{alg}}} \eta_{jL}(u_{jL}^k). \quad (84)$$

Dörfler marking in Algorithm A(III)–(IV), stability (A1), and (84) give

$$\begin{aligned} \theta^{1/2} \eta_{jL}(u_{jL}^k) &\leq \eta_{jL}(\mathcal{M}_{jL}, u_{jL}^k) \stackrel{(A1)}{\leq} \eta_{jL}(\mathcal{M}_{jL}, u_{jL}^*) + C_{\text{stab}} \|u_{jL}^* - u_{jL}^k\| \\ &\stackrel{(84)}{\leq} \eta_{jL}(\mathcal{M}_{jL}, u_{jL}^*) + \lambda \lambda_{\text{opt}}^{-1} \eta_{jL}(u_{jL}^k). \end{aligned}$$

Rearranging the terms, this yields

$$(\theta^{1/2} - \lambda \lambda_{\text{opt}}^{-1}) \eta_{jL}(u_{jL}^k) \leq \eta_{jL}(\mathcal{M}_{jL}, u_{jL}^*). \quad (85)$$

The combination of (55) and (85) implies the following Dörfler criterion for the exact discrete solution u_{jL}^* with parameter $0 < \tilde{\theta} := (\theta^{1/2} - \lambda \lambda_{\text{opt}}^{-1})(1 + \lambda \lambda_{\text{opt}}^{-1})^{-1} < 1$

$$\tilde{\theta} \eta_{jL}(u_{jL}^*) \stackrel{(55)}{\leq} (\theta^{1/2} - \lambda \lambda_{\text{opt}}^{-1}) \eta_{jL}(u_{jL}^k) \stackrel{(85)}{\leq} \eta_{jL}(\mathcal{M}_{jL}, u_{jL}^*) \leq \eta_{jL}(\mathcal{T}_{jL} \setminus \mathcal{T}_{(j+1)L}, u_{jL}^*). \quad (86)$$

Set $a_j := \eta_{jL}(u_{jL}^*)$ and $b_j := C_{\text{stab}} \|u_{(j+1)L}^* - u_{jL}^*\|$. The Dörfler criterion (86) and the argument used for (28) in the proof Lemma 10 yield

$$a_{j+1} \leq q_{\tilde{\theta}} a_j + b_j \quad \text{with } 0 < q_{\tilde{\theta}} := [1 - (1 - q_{\text{red}}^2) \tilde{\theta}]^{1/2} < 1. \quad (87)$$

Quasi-orthogonality (A4) and reliability (A3) show that

$$\sum_{j'=j}^{j+N} b_j^2 \simeq \sum_{j'=j}^{j+N} \|u_{(j+1)L}^* - u_{jL}^*\|^2 \stackrel{(A4)}{\lesssim} (N+1)^{1-\delta} \|u^* - u_{jL}^*\|^2 \stackrel{(A3)}{\lesssim} (N+1)^{1-\delta} a_j. \quad (88)$$

Thus (87)–(88) show that the sequences $(a_j)_{j \in \mathbb{N}_0}$, $(b_j)_{j \in \mathbb{N}_0}$ (extended by zero if $\underline{\ell} < +\infty$) satisfy assumptions (20) of Lemma 9 and thus yields tail summability of $(a_j)_{j \in \mathbb{N}_0}$. Using stability (A1), (84), and equivalence (55) from Lemma 11, it follows that

$$\eta_{jL}(u_{jL}^*) \leq \mathsf{H}_{jL}^k \stackrel{(A1)}{\lesssim} \|u_{jL}^* - u_{jL}^k\| + \eta_{jL}(u_{jL}^k) \stackrel{(84)}{\lesssim} \eta_{jL}(u_{jL}^k) \stackrel{(55)}{\lesssim} \eta_{jL}(u_{jL}^*)$$

and, hence, $\mathsf{H}_{jL}^k \simeq \eta_{jL}(u_{jL}^*) = a_j$ is also tail summable, i.e., there exists a constant $C_{\text{tail}} > 0$ such that, under the change of indices $\ell = jL \in \mathcal{S}$,

$$\sum_{\ell' \in \mathcal{S}, \ell' > \ell} \mathsf{H}_{\ell'}^k \leq C_{\text{tail}} \mathsf{H}_\ell^k \quad \text{for all } \ell \in \mathcal{S}. \quad (89)$$

Finally, the solver contraction (UC) and the smoother stability (US) ensure that

$$\mathsf{H}_\ell^{k'} \leq \begin{cases} \mathsf{H}_\ell^k, & \text{for all } (\ell, k), (\ell, k') \in \mathcal{Q} \text{ with } \ell \in \underline{\mathcal{S}} \text{ and } k \leq k', \\ \max\{1, C_{\text{alg}}^K\} \mathsf{H}_\ell^k, & \text{for all } (\ell, k), (\ell, k') \in \mathcal{Q} \text{ with } \ell \in \mathcal{I} \text{ and } k \leq k'. \end{cases} \quad (90)$$

With tail summability (89) of H_ℓ^k along the solve levels and quasi-monotonicity (90) in k , Steps 2–5 of the proof of Theorem 6 apply to the situation at hand, except that monotonicity (38) is replaced by quasi-monotonicity (90). This concludes the proof. \square

TU WIEN, INSTITUTE OF ANALYSIS AND SCIENTIFIC COMPUTING, WIEDNER HAUPTSTRASSE 8–10, 1040,
AUSTRIA

Email address: philipp.bringmann@asc.tuwien.ac.at

Email address: christoph.lietz@asc.tuwien.ac.at (corresponding author)

Email address: dirk.praetorius@asc.tuwien.ac.at